This dissertation has been
microfilmed exactly as received 67-15,895

JOHNSON, Robert Marland, 1939-
THE RELATION BETWEEN SURFACE DAMAGE AND FILM STRENGTHENING EFFECTS.

The University of Oklahoma, Ph.D., 1967
Engineering, metallurgy

University Microfilms, Inc., Ann Arbor, Michigan

Downloaded from SHAREOK. Persistent Handle URL: https://hdl.handle.net/11244/2244

THE UNIVERSITY OF OKLAHOMA

GRADUATE COLLEGE

THE RELATION BETWEEN SURFACE DAMAGE AND FILM STRENGTHENING EFFECTS

A DISSERTATION

SUBMITTED TO THE GRADUATE FACULTY

in partial fulfillment of the requirements for the

degree of

DOCTOR OF PHILOSOPHY

BY

ROBERT MARLAND JOHNSON

Norman, Oklahoma

1967

THE RELATION BETWEEN SURFACE DAMAGE

AND FILM STRENGTHENING EFFECTS

APPROVED BY

DISSERTATION COMMITTEE

ABSTRACT

The strengthening effects produced by various metallic coatings on copper single-crystals were studied. There was no relation between the magnitude of the strengthening produced and the mechanical strength of the various coatings. On this basis, a mechanism involving the operation of the coating as a simple barrier to dislocation egress from the crystal was considered inappropriate. Likewise, there was no relation between the relative shear moduli of coating and substrate and the strengthening produced. Thus, the elastic repulsion of dislocations from the coating-substrate interface was also considered to be unimportant as a mechanism. None of the results suggested that the suppression of surface Frank-Read sources made an important contribution to the strengthening effect.

Significant film strengthening effects were always accompanied by cracking of the coating either prior to or during deformation. An increase in dislocation density at the substrate surface was associated with film cracking. This surface damage which resulted from residual stresses in the coating is believed to be an important factor in producing the film strengthening effects which were observed.

ACKNOWLEDGEMENT

I sincerely wish to thank Dr. Robert J. Block for his fine guidance and help throughout the course of this investigation.

I am greatly indebted to my wife, Mary, for her patience and understanding over the years.

Also my gratitude is expressed to Messrs. Richard V. Feaster and Michael W. Lewis for the assistance they gave me in the performance of various aspects of the work.

Finally, I wish to express appreciation to the Atomic Energy Commission for its support of this investigation and to the National Aeronautics and Space Administration for the fellowship I received early in my graduate studies.

TABLE OF CONTENTS

	Page
LIST OF TABLES	vi
LIST OF ILLUSTRATIONS	vii
Chapter	
I. INTRODUCTION	1
II. EXPERIMENTAL WORK	7
III. RESULTS AND DISCUSSION	14
Reproducibility of Tension Tests	14
Effects of Various Coatings	17
Coating Strength Dependence	20
Surface Source Theory	23
Residual Stress Effects	24
Behavior of the Coating during Deformation	43
IV. CONCLUSIONS	63
BIBLIOGRAPHY	64
APPENDICES	
A. STRESS-STRAIN PARAMETERS FOR COATED AND UNCOATED CRYSTALS	67
B. THE MORPHOLOGY OF SEVERAL COATINGS	69

LIST OF TABLES

Table		Page
1.	Orientations of Crystals	10
2.	Characteristics of Electroplated Coatings	12
3.	Residual Stresses in Electroplated Coatings	13
4.	Atomic Sizes and Morphology of Coatings	42

LIST OF ILLUSTRATIONS

Figure		Page
1.	Geometric Representation and Sterographic Plot of the Orientation of the Crystals Used	8
2.	Idealized Representation of the Stress-Strain Curves Obtained from Copper Crystals	15
3.	Stress-Strain Curves for Uncoated Specimens Indicating The Effect of Subgrain Size (After Block)	16
4.	Stress-Strain Curves for Uncoated Specimens Indicating The Effect of Subgrain Size	18
5.	Stress-Strain Curves for Coated Specimens Indicating The Effect of Various Coatings	19
6.	Schematic Diagrams of Ways in Which a Film May Accommodate Slip in the Substrate	22
7.	Stress-Strain Curves for a Specimen with a 125 Å Vapor Deposited Cr Film and for an Uncoated Specimen	25
8a.	A Representative Area of a Specimen Etched to Reveal Dislocations	27
8b.	Same Area Shown in Figure 8a After Plating with 0.5 Micron Cr, Removing the Plate in HCl, Polishing Away a 1 Micron Layer of Cu and Etching to Reveal Dislocations	28
8c.	Same Area as in Figure 8a After Removal of 2 Microns of Cu and Reetching	29
8d.	Same Area as in Figure 8a After Removal of 3 Microns of Cu and Reetching	30
9.	Stress-Strain Curve for a Specimen Electroplated with 0.8 Micron of Cr and Then the Cr Removed in HCl Before Testing	32
10a.	Specimen Coated with 125 Å Cr by Vapor Deposition	34
10b.	Same Area as Figure 10a After Cr Removed in HCl and the Specimen Reetched	35

Figure		Page
10c.	Higher Magnification of Specimen in Figure 10b	36
11.	Surface of a Crystal Electroplated with a 1 Micron Coating of Re, the Coating Then Removed in H_2O_2 and the Crystal Etched to Reveal Dislocations	37
12.	Damaged Surface of a Crystal Electroplated with 1.7 Micron Coating of Rh Over a 500 Å Flash of Re	39
13.	Damaged Surface of a Crystal Electroplated with 1.7 Micron Coating of Cr Over a 500 Å Flash of Re	40
14a.	(111) Surface of a Crystal Coated with 1 Micron Re and Strained to 8% Shear	44
14b.	Higher Magnification of Same Area Shown in Figure 14a . . .	45
15.	Surface of a Crystal Coated with 1 Micron of Ru and Strained to 4.5% Shear	47
16.	Curves Showing the Stress Levels in the Various Coatings as a Function of Substrate Shear Strain	48
17a.	Substrate Damage Beneath the Cracks in a 1 Micron Cr Film	50
17b.	Same Specimen as Shown in Figure 17a at Higher Magnification	51
18a.	Substrate Damage Beneath Cracks in a 1 Micron Re Film . . .	53
18b.	Same Specimen as Shown in Figure 18a at Higher Magnification	54
19.	Load-Extension Curves for a Specimen with a 125 Å Vapor Deposited Cr Coating, a Specimen with a 0.8 Micron Electroplated Cr Coating Which Was Removed Before Testing, a Specimen with a 0.8 Micron Electroplated Cr Coating, and an Uncoated Specimen	56
20.	Surface of a Crystal Tested into Stage III with a 125 Å Vapor Deposit of Cr.	58
21.	Surface of a Crystal Tested into Stage III with a 1 Micron Cr Electroplate	59
22.	Stress-Strain Curves for Specimens of the Same Crystal Having Cr Coatings of Various Thicknesses (After Block) . .	62

THE RELATION BETWEEN SURFACE DAMAGE AND FILM STRENGTHENING EFFECTS

CHAPTER I

INTRODUCTION

Surface conditions can strongly influence plastic deformation in metals. In single crystals the critical resolved shear stress, strain hardening rate, stress for twinning, fatigue behavior, fracture and other properties have been observed to be dependent on the state of the surface. These effects have been adequately reviewed in two recent articles (1, 2).

Strengthening by a thin film was first observed by Roscoe (3) using cadmium single crystals. It was found that oxide coatings of less than 20 atoms thick not only increased the critical resolved shear stress but also the flow stress after deformation had proceeded. Cracking of the film was noted during deformation. Since the oxide coating was too thin to support an appreciable portion of the applied stress, it was concluded that more was involved than simply the strength of the oxide film alone.

Roscoe's work was confirmed by Cottrell and Gibbons using cadmium (4). Similar effects with oxide and hydroxide films have been reported for aluminum (5, 6), zinc (7), and silver (8). Other investigators have examined the effects produced by metallic films

on single crystals of zinc (9, 10, 11), tin (10), lead (10), cadmium (12), silver (13), and copper (14, 15, 16).

In the body of experimental data indicating the existence of film strengthening effects there is confusion and often contradiction as to which of the strength parameters are affected and in what way. For example, it has been reported that thin surface films did not affect the initial flow stress significantly but did increase the strain hardening rate (7, 8, 10). In contrast, Lipsett and King (12) found that the CRSS was raised but there was little effect on the strain hardening rate. Lipsett and King (12) also indicated that the surface effects were independent of film thickness but dependent on the orientation. However, in their experiments Gilman and Read (9) found that the magnitude of the surface effects were dependent on film thickness.

The abnormal torsional after-effect experiments of Barrett et al (17, 18) provided a mechanism capable of explaining film strengthening effects. The coating was pictured as a mechanical barrier to the egress of dislocations generated within the substrate crystal and moving toward the surface. The dislocations become arranged in pile-ups against the coating-substrate interface. Perhaps the simplicity and intuitive appeal of this mechanism are responsible for an acceptance which has persisted even though the experiments which yielded it have been questioned (19). According to this mechanism one might expect the magnitude of the film strengthening effect to be closely related to the mechanical strength of the coating.

A mechanical interaction of the coating with approaching dislocations such as discussed above is not the only possibility which

exists. Head (20) and Cottrell (21) pointed out that the coating could influence dislocation motion through its effects on the stress field which surrounds the dislocation. In the presence of a coating of lower shear modulus than the substrate crystal, dislocations are attracted toward the coating-substrate interface. The equivalent is true in the absence of a coating at the surface. However, if the coating has a higher shear modulus than that of the substrate crystal, dislocations will seek an equilibrium position at some distance away from the coating-substrate interface. This distance depends upon the ratio of the shear moduli of the coating and substrate, and the thickness of the coating. This mechanism also might be expected to produce dislocation pile-ups but the strengthening effect on a given substrate should depend upon the shear modulus of the coating.

A third mechanism which might produce the observed strengthening effects is concerned with the onset of plastic deformation in crystals. Several articles review theories of work hardening in crystals (21, 22, 23, 24). As implied by Young (25) the onset of plastic deformation is associated with the multiplication of dislocation line lengths acting as Frank-Read sources. The stress required to activate a dislocation segment as a Frank-Read source is inversely proportional to its length. Considering this Fisher (26) suggested that a dislocation which terminates in the surface, because of the image force acting on the free end, should behave as though it had twice the effective length as that of an equivalent segment lying entirely within the crystal. Thus the onset of plastic deformation may be associated with the activation of these long surface sources.

The presence of a coating may serve to pin the free end of the surface source raising if not doubling the critical resolved shear stress. If this mechanism operates, the critical resolved shear stress should be thickness independent since presumably very thin coatings could produce the required pinning. While there is some direct experimental evidence that surface sources are important to the onset of plastic deformation (27), a doubling of the critical resolved shear stress has not been generally observed.

There are other mechanisms through which a coating might interact with dislocations terminating in the surface. Gilman (28) proposed that a coating would tend to restrain the ability of a screw dislocation nearly normal to the surface to cross slip. Multiplication of dislocations by cross slip of screw dislocations and dislocation dipole formation thus may be inhibited by surface coatings.

Closely associated with defining the effect of surface conditions on mechanical behavior is the problem of preferred or enhanced deformation near the surface. In a series of experiments, Kramer et al (20, 30, 31) demonstrated that surface removal during deformation promotes long easy glide in aluminum. Other workers have observed examples of heterogeneous surface deformation (10, 32, 33). Nakada and Chalmers (34) in their micropeening experiments found that the extent of easy glide could be affected by the thickness of a work hardened layer at the surface.

The mechanism accounting for the effects produced by preferential work hardening at the surface involves the activation of secondary slip systems and dislocation tangle formation. According to Nakada and

Chalmers (34) dislocations approaching the damaged layer tend to form pile-ups which impede their motion toward the surface. Using deformed aluminum crystals with an oxide coating, Nakada and Chalmers demonstrated the existence of preferential work hardening in a surface layer about 10 microns thick. In the absence of any direct evidence, they attributed the damaged layer to the piling up of primary dislocations beneath the oxide coating. Other observations have been made which indicate the existence of a preferentially deformed layer beneath the surface coating (10). The effect of a damaged layer may well be the production of dislocation tangles. However, the mechanism which is responsible for the damaged layer itself, which is the crux of the film strengthening mechanism has not been clearly demonstrated.

The present investigation was designed to verify experimentally the several film strengthening mechanisms which have been proposed. The results of tension tests using selected metallic coatings on single crystal substrates have been used to indicate which of the coating parameters are important in producing large strengthening effects. A regular dependence on the shear modulus of the coating would tend to favor the elastic repulsion mechanism. A similar dependence on the strength of the coating (as indicated by its hardness) would indicate the operation of a mechanical barrier mechanism. The importance of surface dislocation sources should be revealed by the behavior of the critical resolved shear stress in the presence of the various coatings.

Throughout the study the role of other film characteristics, traditionally ignored, such as adherence, state of residual stress, and

behavior during deformation were considered in relation to magnitude of the film strengthening effect.

CHAPTER II

EXPERIMENTAL WORK

The present investigation was carried out using copper single crystals as the substrate material. Electroplated and, in one case, evaporated metal films were used as coatings. Coatings were chosen on the basis of strength and shear modulus relative to the substrate copper. The use of copper single crystals provided several distinct advantages. It has been rather thoroughly studied in the uncoated state by other workers (35, 36, 37, 16). Copper shows negligible static recovery or annealing at room temperature. Of particular importance was the availability of dislocation etches for copper. Dislocation densities obtained from etch pit counts have been correlated to the flow stress by several workers (38, 39, 40). Previous work by Garstone et al (14) and Block (16) indicated which coatings might be expected to produce large effects and the general nature of these effects.

The copper crystals grown for this study were oriented for long easy glide as shown in Figure 1. Theory (21, 41) and experiment (42) indicated that larger surface effects occur in easy glide rather than in the later stages of deformation.

The parallel (111) surfaces were chosen to contain the slip vector of the primary slip system. It has been shown that dislocations can be reliably etched in copper if the surface is within a few degrees

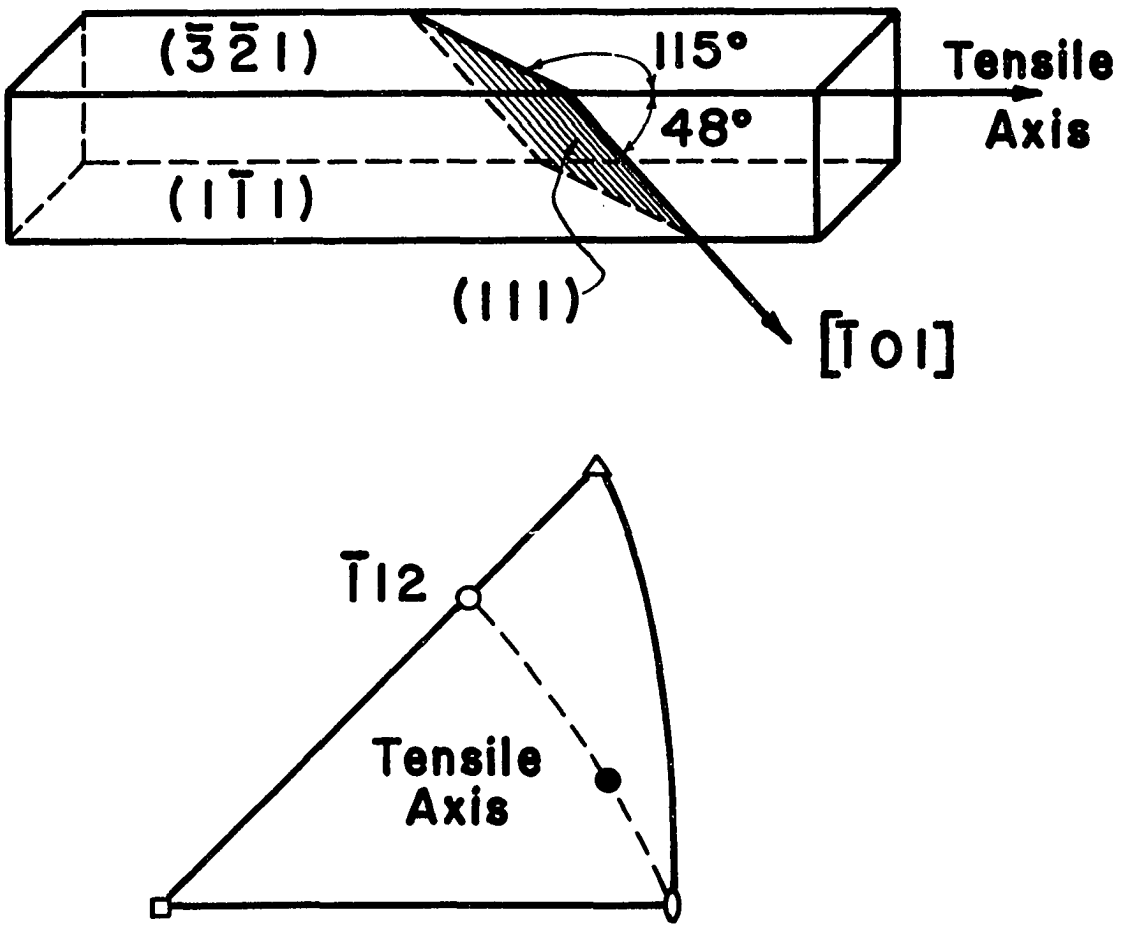


FIGURE 1

GEOMETRIC REPRESENTATION AND STEREOGRAPHIC PLOT OF THE ORIENTATION OF THE CRYSTALS USED

of (111) (38, 43, 44). With the particular orientation used the surface remained in the (111) orientation throughout easy glide.

Single crystals were grown from ASARCO 99.999% copper using a modified Bridgeman technique and a multiple cavity mold of spectroscopically pure graphite. A novel seeding technique was used to join each of the six cavities of the mold to a common seed. In this procedure a copper seed crystal of the desired orientation was placed in one cavity and then copper wires attached to the seed were run into the other cavities. These wires carried the orientation of the seed to each cavity during the solidification process. Crystals grown in cavities joined to the seed by the wires were observed to contain fewer subgrain boundaries than crystals grown directly from the seed. Crystal growth was carried out in a quartz capsule under a static vacuum of less than 10^{-5} torr.

In the as-grown condition the crystals were of square cross section 1/8 inch on a side and 10 inches long. After growth the crystals were carefully removed from the mold and their orientation established by the Laue back reflection technique. The orientations of the crystals utilized in this study are presented in Table 1.

Acceptable crystals were cut with an acid saw and coded according to the following scheme. Sample 34D4 indicates the 34th batch, cavity D of the mold and the fourth piece from the top of the crystal. After cutting, the crystals were annealed in order to lower their dislocation content. The treatment consisted of holding the crystals for 24 hours at a temperature of $1050^{\circ}C$ under a dynamic vacuum of 10^{-5} torr followed by cooling to room temperature over a 20-hour period.

TABLE 1

ORIENTATIONS OF CRYSTALS

Crystal	λ_0	φ_0	Schmid Factor m
33F	43°	50°	.470
34B	49°	45°	.464
34C	49°	50°	.421
34D	49°	45°	.464
34F	49°	45°	.464
35F	46°	47°	.474
38B	55°	39.5°	.443
38C	46°	46°	.443
38E	49°	45°	.464
40E	52°	41°	.465

In order to reveal dislocations the specimens were polished in a solution of equal parts acetic acid, nitric acid and orthophosphoric acid and then etched using a variation of Livingston's reagent (45). The proportions in the etch solution were 1 ml bromine, 15 ml glacial acetic acid, 25 ml concentrated hydrochloric acid, and 90 ml distilled water. Etch pits appeared as triangular black spots on the (111) faces.

The cut and annealed crystals were converted into tension test specimens by soldering 5/16 inch steel balls on each end. The soft solder, 61.5% tin, 35% lead, 3% silver was used for this purpose because

of its low melting temperature and its relatively high creep resistance. The specimens were prepared with a guage length of approximately one inch free from grip constraints.

Tension testing was accomplished using specially machined grips which accepted the steel balls on the specimen. Axiality was achieved through the use of a positive alignment jig. These procedures permitted interruption of tests and specimen removal without evidence of bending or other anomalies after the specimen was reinserted into the grips and the test resumed.

Crystals tested in the unplated condition were chemically polished, dipped in 10% orthophosphoric acid, rinsed in distilled water, held in a 5% potassium cyanide solution for 15 seconds, rinsed again and then dried with absolute methyl alcohol. This procedure, according to Reddy and Wilman (46), was found to leave the copper surface bright and free from any surface film that could be detected by electron diffraction methods.

Coatings used in this study were usually applied by electro-deposition from commercial proprietary plating solutions. Table 2 indicates the various coatings, the source of the plating bath and the pertinent properties. The thicknesses of the electroplated films were predetermined from current efficiency studies using a weight gain measurement.

Tension testing was carried out immediately after cleaning or plating in an Instron tensile testing machine using an extension rate of 0.002 inch per minute (as cross head movement). The cross sectional area and length of every specimen was measured before testing. Machine

TABLE 2

CHARACTERISTICS OF ELECTROPLATED COATINGS

Coating	Source	Shear Modulus gm/mm^2	Hardness
Lead	Fluoborate Bath	0.56×10^6	Very low
Gold	Industrial 24 Kt Gold (Technic, Inc.)	2.8×10^6	80 Knoop*
Copper	Sulfate Bath	4.9×10^6	80 Knoop*
Chromium	Unichrome CF-500 (M & T Chemicals)	7.4×10^6	800 DPH**
Rhodium	Rhodium Sulfate TP (Technic, Inc.)	15.6×10^6	800 DPH#
Ruthenium	Ruthenium TP (Technic, Inc.)	17.5×10^6	650 Knoop#
Rhenium	Rhenium-A (Technic, Inc.)	27.5×10^6	360 Knoop#

* Bulk Property
\# Supplied by manufacturer
**Measured value

plotted load-extension curves were converted to resolved shear stress-resolved shear strain curves using the standard relations (47).

In certain cases it was found desirable to remove the coating in order to examine the dislocation arrangements beneath the film. Chromium was removed in a dilute hydrochloric acid solution without detectible

attack of the copper substrate. Rhenium and lead were dissolved in 3% hydrogen peroxide which likewise did not attack the substrate. When removal of other coatings was required, such as ruthenium, rhodium, and gold, they were applied over a 500 Å rhenium flash and stripped in hydrogen peroxide.

Residual stresses in several electroplates were measured by the beam deflection method of Brenner and Senderoff (48). Either copper or 302 stainless steel sheet 0.003 inch thick was used as a substrate. The values obtained are presented in Table 3.

TABLE 3

RESIDUAL STRESSES IN ELECTROPLATED COATINGS

Coating	Substrate	Observed Stress Psi	Type
Gold	Copper	Very low	----
Chromium	Copper	7970	Tension
Chromium	Stainless Steel	7080	Tension
Rhodium	Copper	4150	Tension
Ruthenium	Copper	5560	Tension
Rhenium	Copper	1860	Tension

CHAPTER III

RESULTS AND DISCUSSION

The results of the mechanical tests are presented as resolved shear stress-resolved shear strain curves. Parameters were determined from the stress-strain curves according to Figure 2. The critical resolved shear stress, τ_0, was defined as the intersection of an extrapolation of the linear portion of easy glide and an extrapolation of the elastic response. In order to permit comparison of stress-strain curves early in the plastic region a stress value, τ_{00}, defined at a shear strain of 2×10^{-4} was found to be useful. The extent of easy glide, a_2, and the stress at the end of easy glide, τ_2, were taken at the intersection of the extrapolation of the linear portions of Stage I and Stage II. τ_3, the stress at the end of Stage II, was taken at the deviation of the curve from the linear portion of Stage II. The slopes of easy glide and linear hardening, stages I and II, are represented as θ_I and θ_{II} respectively.

Reproducibility of Tension Tests

Using identical test procedures, Block (16) has demonstrated that reproducibility of tests among 99.999% copper crystals having the same orientation and surface treatment is dependent upon substructure. Figure 3, taken from this work, indicates a variation of flow stress in easy glide of less than 15 gm/mm^2 among crystals having an average

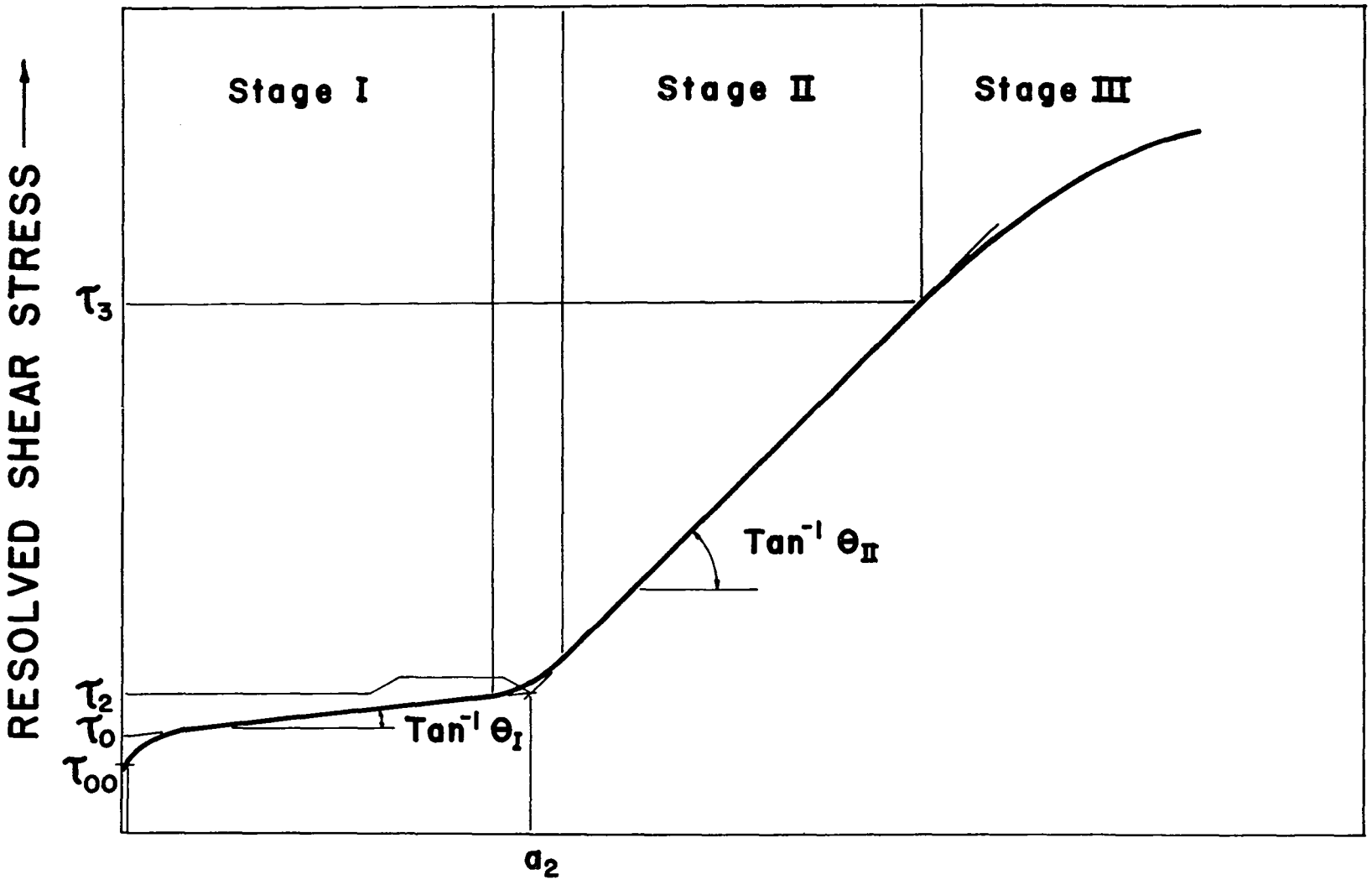


FIGURE 2

IDEALIZED REPRESENTATION OF THE STRESS-STRAIN CURVES OBTAINED FROM COPPER CRYSTALS. The stages of plastic flow and the deformation parameters are indicated. τ_{00} is taken at a shear of 2×10^{-4}.

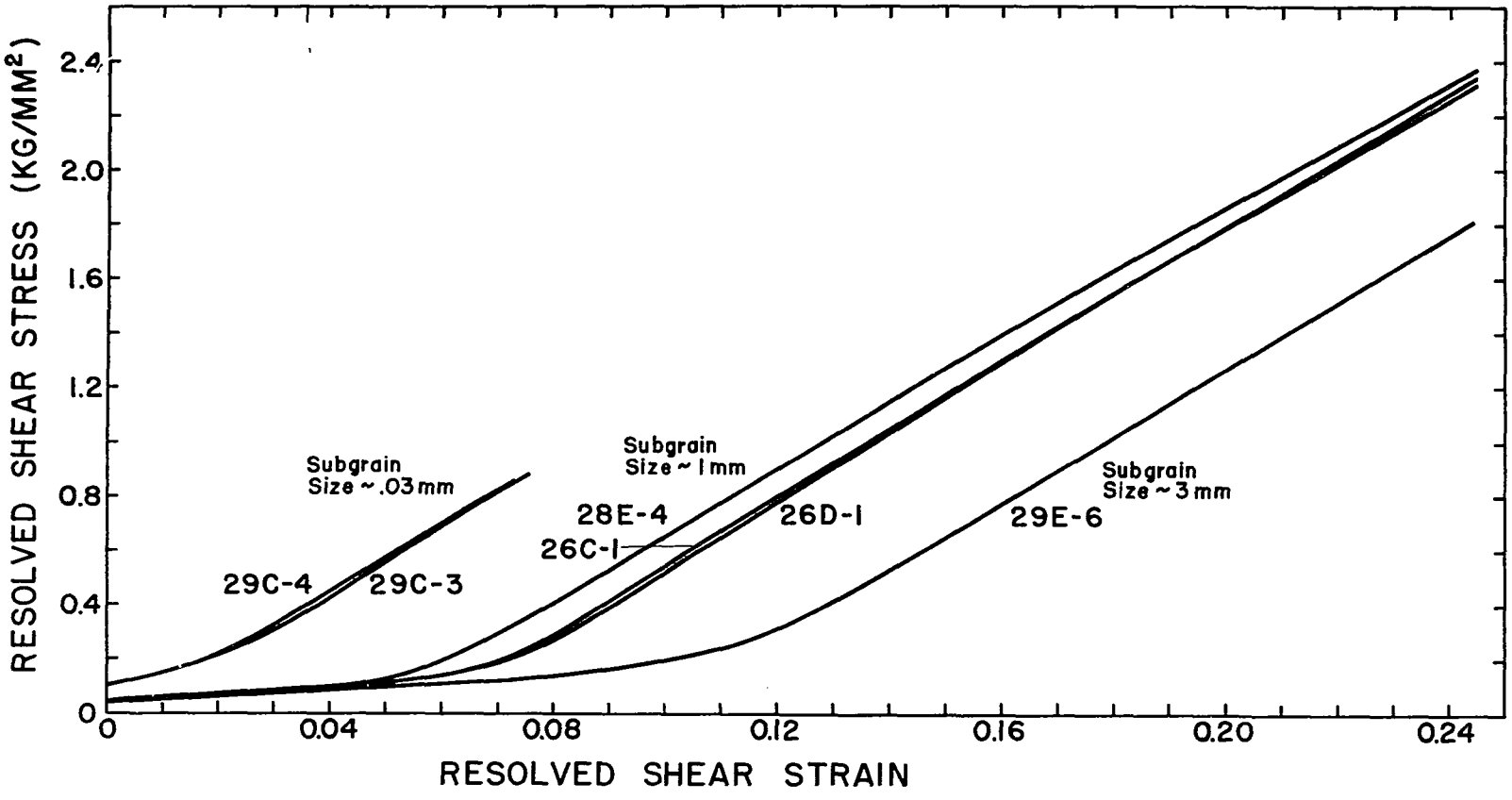


FIGURE 3

STRESS-STRAIN CURVES FOR UNCOATED SPECIMENS INDICATING THE EFFECT OF SUBGRAIN SIZE
(After Block)-(16)

subgrain diameter greater than 1 mm. In the present work the results of a more detailed study of the question of reproducibility in easy glide are presented in Figure 4. These curves indicate that in general Stage I is lower and longer for combinations involving low initial dislocation density and large subgrain size, the latter being more important. The dependency of the flow stress τ_{00} (at 2×10^{-4} shear), on subgrain size for these uncoated crystals has been found to fit the empirical relation $\tau_{00} = (5.45/x) + 16.3$ where x is the subgrain size in mm and τ_{00} is given in gm/mm^2. The data of Figure 3 are consistent with this relationship. Throughout the present work comparisons have been made among crystals having approximately the same subgrain size.

Effects of Various Coatings

The strengthening effects produced by electroplated coatings of lead, gold, copper, chromium, rhodium, ruthenium, and rhenium are shown in the curves of Figure 5. A stress-strain curve for an uncoated crystal is provided for reference. Appendix A lists values of particular parameters taken from the stress-strain curves for plated and unplated crystals. $\tau_{00_{cal}}$ is a calculated value for the flow stress at 2×10^{-4} shear from the empirical formula given above, $\tau_{00} - \tau_{00_{cal}}$ is a measure of the increase in initial flow stress of the plated crystal compared with that of an unplated crystal. $\tau_0 - \tau_{00_{cal}}$ is a measure of the strain hardening rate before the linear portion of Stage I is achieved. $\theta_I/\theta_{I\ unplated}$ is the ratio of the slope of easy glide for a particular crystal to the average slope of easy glide for all unplated crystals.

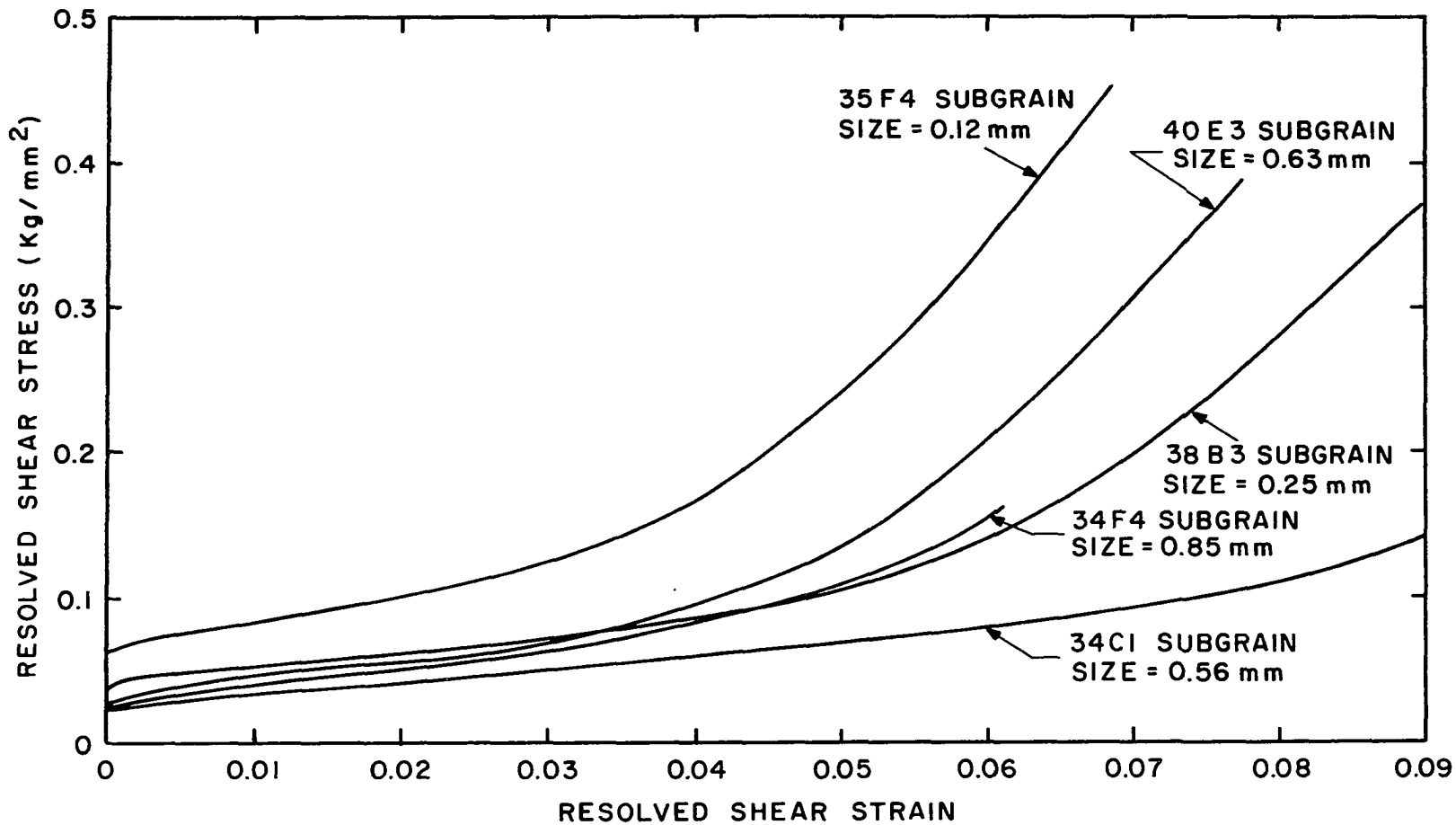


FIGURE 4

STRESS-STRAIN CURVES FOR UNCOATED SPECIMENS INDICATING
THE EFFECT OF SUBGRAIN SIZE

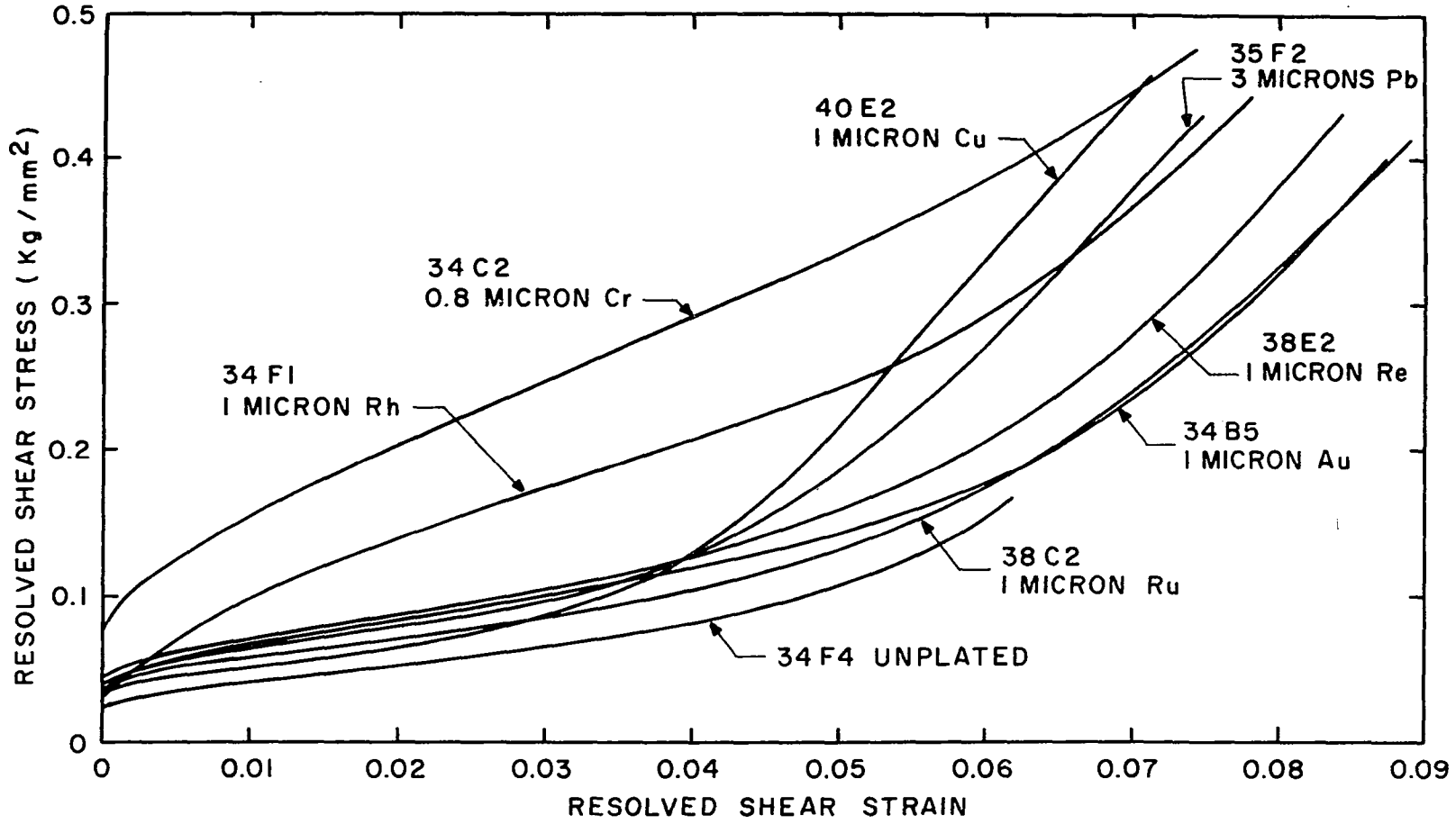


FIGURE 5

STRESS-STRAIN CURVES FOR COATED SPECIMENS INDICATING THE EFFECT OF VARIOUS COATINGS. The curve for an uncoated specimen is included for comparison.

The curves of Figure 5 show no regular relationship between the shear modulus of the coating and the strengthening it produces. Average shear moduli for the various coatings are presented in Table 2. Rhenium and ruthenium have the highest shear moduli of all of the coatings used. However, the general strengthening in Stage I produced by 1 micron deposits was approximately the same as obtained with gold and copper coatings of the same thickness and a lead coating 3 microns thick. The only large strengthening effects were observed with a 1 micron coating of rhodium and a chromium coating slightly less than 1 micron thick. The absence of a shear modulus dependency was implied by Garstone, Honeycombe, and Greetham (14) in their tests of chromium and nickel coatings on a copper crystal. Both chromium and nickel have approximately the same elastic modulus. However, no strengthening effect was observed with the nickel coating while a substantial strengthening was produced by the chromium coating. In the absence of any dependence upon the shear modulus of the coating, mechanisms which involve elastic repulsion of dislocations from the coating-substrate interface appear to be unimportant as a cause of the strengthening due to surface films which has been observed.

Coating Strength Dependence

In order to consider the ability of a coating to inhibit plastic deformation in the substrate, a mechanism for the manner in which the coating accommodates slip in the substrate must be assumed. This process is neither completely obvious nor necessarily the same for all films. It would appear that the mechanical strength of the coating should be

of particular importance. However, the adherence to the substrate and whether the coating is ductile or brittle may also be important considerations. Figure 6 illustrates three different mechanisms by which a coating might accommodate plastic deformation of the substrate. In case (a) the coating is considered to fracture brittlely (Figure 6a) allowing the dislocations generated within the substrate to move out of the crystal at the exposed slip plane trace. Case (b) considers a coating which is not strongly adherent so that it may detach during deformation (Figure 6b). It has been shown (49) that once detachment begins it may be expected to occur over large areas with fracture occurring later in the deformation or not at all. The final situation, case (c), involves shear in the coating (Figure 6c). Obviously, epitaxial coatings will behave differently from polycrystalline coatings. Brame and Evans (13) have thoroughly considered the mechanism by which dislocations move from a substrate crystal through an epitaxial coating of different lattice parameter. They conclude that as lattice misfit increases shear of the coating tends to become difficult and brittle fracture is more likely to occur.

The situation described in Figure 6c is simplified conceptually if the coating is not epitaxial. Dislocations generated in the substrate are accommodated in the boundary between substrate and coating in much the same way that they are accommodated in grain boundaries during plastic deformation of polycrystalline aggregates. The accommodation induces shear in the coating which results in a step at the surface.

Large scale detachment was only observed for rhenium coatings. For all other coatings either case (a) or case (c) will apply. In both

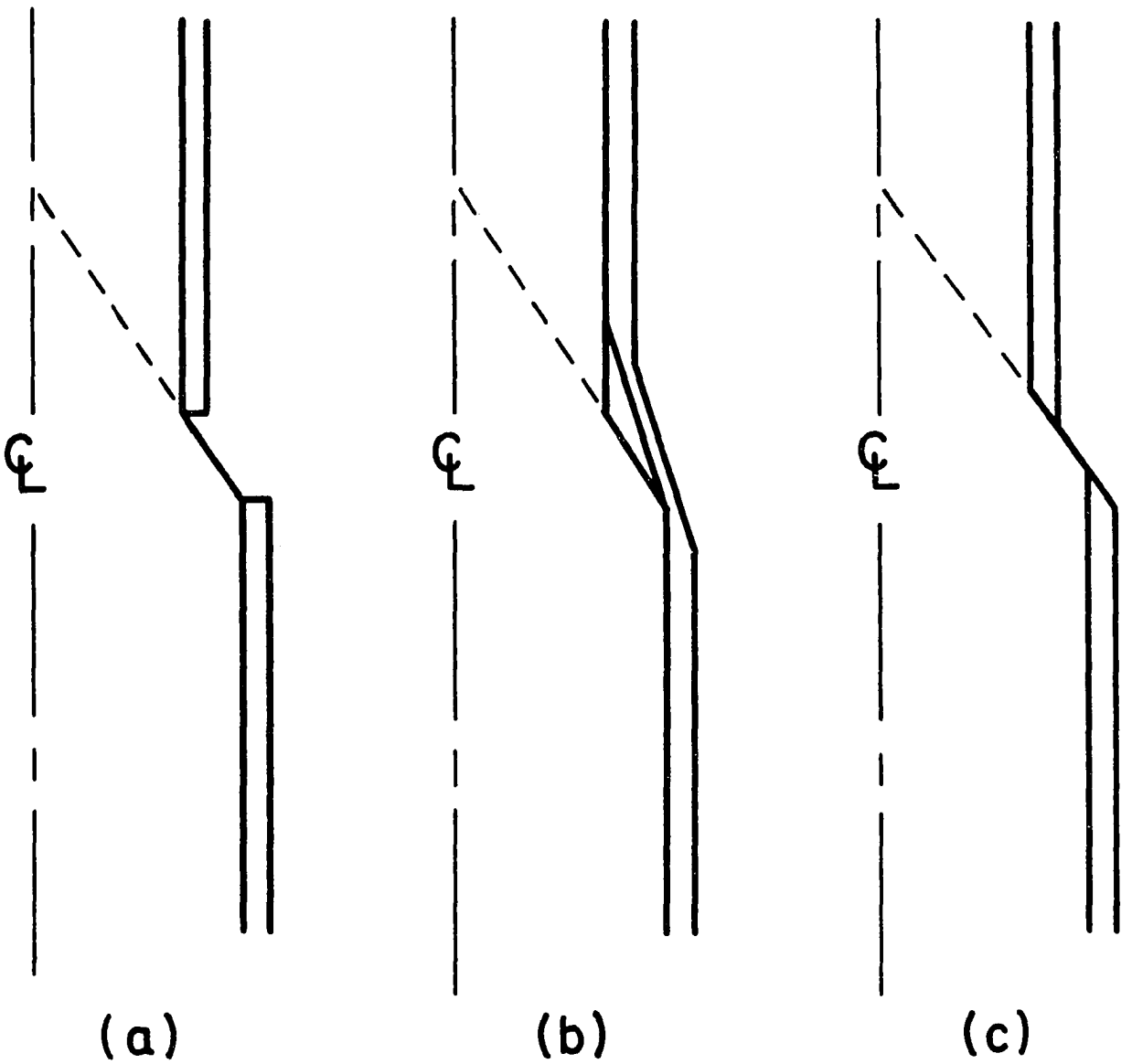


FIGURE 6

SCHEMATIC DIAGRAMS OF WAYS IN WHICH A FILM MAY ACCOMMODATE SLIP IN THE SUBSTRATE

(a) Film cracks along slip traces
(b) Film is initially detached without cracking
(c) Film shears off

of these cases the mechanical strength of the coating should measure its ability to inhibit deformation of the substrate crystal. Reliable measurement of the mechanical strengths of thin films is difficult and was not attempted. Instead, the relative strengths of the various coatings were judged from their hardness. Hardness values for the various coatings are presented in Table 2.

The magnitude of the strengthening produced by the coatings tested (Figure 5) did not appear to depend systematically upon the hardness of the coatings used. Chromium, which was the hardest coating tested, did produce the largest effect. Likewise, rhodium, which is quite hard, showed considerable strengthening. However, among rhenium, gold, copper, and lead there is considerable variation in hardness without a corresponding variation in the strengthening produced.

Surface Source Theory

Without exception the critical resolved shear stress of the coated crystals is significantly greater than that for the unplated crystals (Figure 5). Only for the tests of crystals having 1 micron of gold, 1 micron of rhenium, and 3 microns of lead is there approximately a doubling of the critical resolved shear stress as required by theory. In the experiment regarded as proof of the surface source theory, Adams (27) did not report that the critical resolved shear stress was doubled for his high zinc alloy coatings.

A crystal was prepared with a 125 Å chromium coating which was applied by vapor deposition on an unheated substrate. The chamber pressure was less than 5×10^{-6} torr during evaporation. A stress-strain

curve for this specimen and an uncoated crystal are presented in Figure 7. It is certainly to be expected that a chromium coating of this thickness should be sufficient to anchor the free ends of surface sources. However, the critical resolved shear stress was virtually unaffected. These results demonstrate that the effect of coatings on surface dislocation sources is not of major importance in producing the observed strengthening effects.

Residual Stress Effects

The lack of a simple relationship between the strengthening observed and either the shear moduli or the hardness of the coatings studied, invited a more careful consideration of other film parameters. It is well known that electro-deposited or evaporated coatings are seldom free from residual stresses. In order to determine whether these stresses played a role in producing the effects which were observed, the following experiment was carried out.

A copper crystal was chemically polished and etched to reveal dislocations. A representative area of the etched crystal is shown in Figure 8a. Dislocations were arranged in subgrain boundaries and scattered within the subgrains. The dark shadows which appear on the photomicrographs are caused by undulations in the surface. After polishing, the crystal was electroplated with a 0.5 micron chromium coating which was immediately removed in hydrochloric acid. This was followed by chemical polishing which removed approximately a 1 micron layer of copper from the surface; the crystal was again etched to reveal dislocations. Figure 8b shows the same area as Figure 8a after the plating and removal treatment.

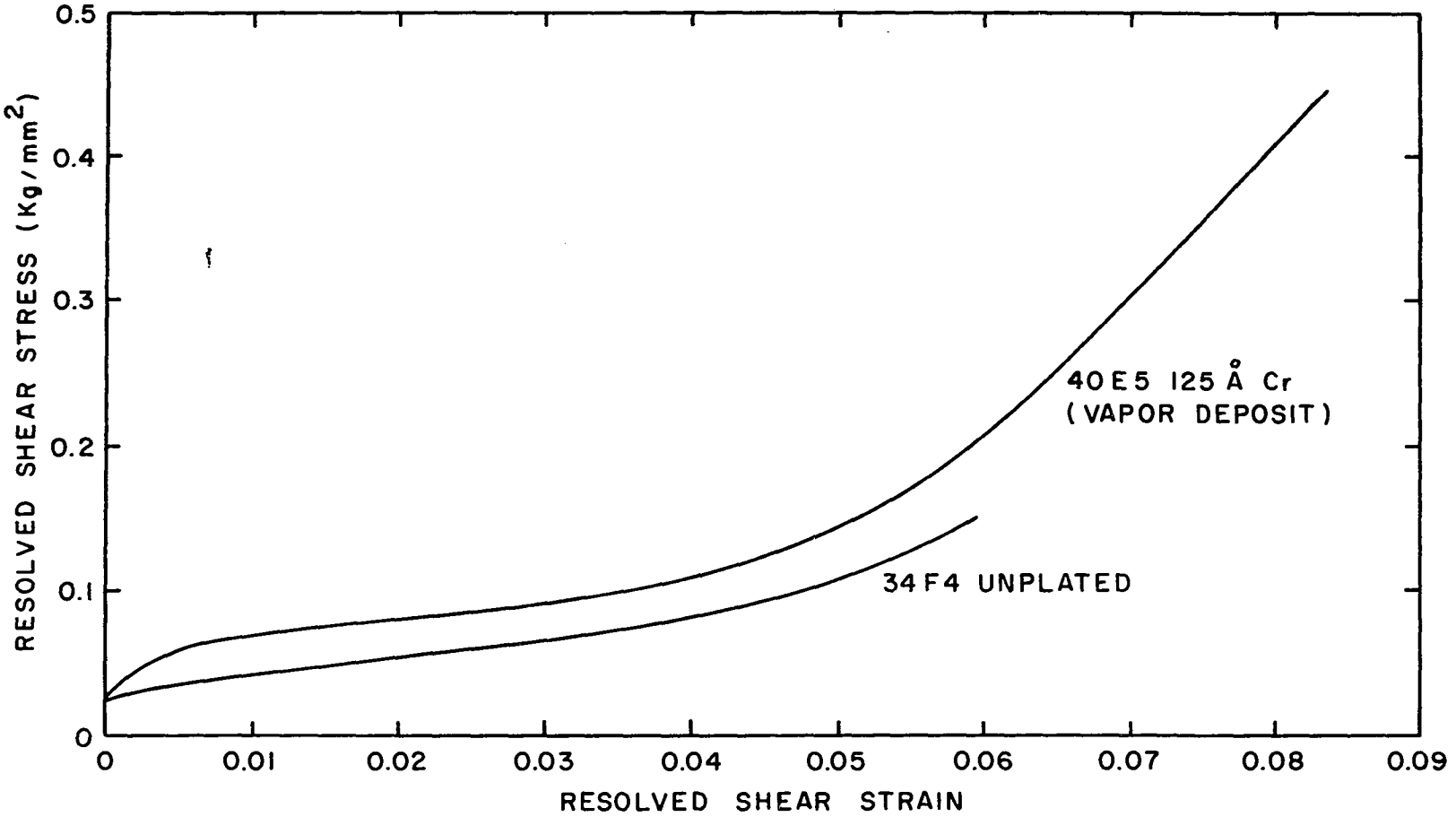


FIGURE 7

STRESS-STRAIN CURVES FOR A SPECIMEN WITH A 125 Å VAPOR DEPOSITED Cr FILM AND FOR AN UNCOATED SPECIMEN

The broad dark lines and the areas immediately adjacent show extremely high dislocation densities indicating that the substrate crystal has undergone localized plastic deformation. These lines are believed to be evidence of cracks resulting from residual stresses in the electro-deposit. The formation of these cracks tends to relieve stresses in the coating and causes shear in the substrate near the substrate-coating interface. Continued removal of copper from the surface by chemical polishing revealed the depth to which this damage extended. Figure 8c shows the same area as in the previous photomicrograph after removal of approximately 2 microns of copper from the surface of the crystal. The density of dislocations beneath and adjacent to the crack traces is considerably lower than in the previous photomicrographs. The clusters of fine lines which are in evidence in this photomicrograph and the next are due to terracing of the surface caused by the prolonged chemical polishing. Figure 8d shows the surface after 3 microns of copper have been removed. Some of the damage due to cracking of the coating has disappeared at this depth. In many large areas the dislocation density is equivalent to the initial density before electroplating. It was established that the damage due to a 0.5 micron chromium coating extended approximately 5 microns below the coating-substrate interface.

The existence of surface damage as a result of the application of a surface coating appears to be an important consideration. Westwood (50) presented photomicrographs of lithium fluoride having a reacted magnesium oxide surface layer. Beneath this surface layer an excess of dislocations was observed and attributed to pile-ups. However, the



FIGURE 8a

A REPRESENTATIVE AREA OF A SPECIMEN ETCHED TO REVEAL DISLOCATIONS. 50X



FIGURE 8b

SAME AREA SHOWN IN FIGURE 8a AFTER PLATING WITH 0.5 MICRON Cr, REMOVING THE PLATE IN HCl, POLISHING AWAY A 1 MICRON LAYER OF Cu AND ETCHING TO REVEAL DISLOCATIONS. 50X



FIGURE 8c

SAME AREA AS IN FIGURE 8a AFTER REMOVAL OF 2 MICRONS OF Cu AND REETCHING. 50X



FIGURE 8d

SAME AREA AS IN FIGURE 8a AFTER REMOVAL OF 3 MICRONS OF Cu AND REETCHING. 50X

arrangement may have been induced in the substrate as a result of stresses set up during production of the surface coating.

The degree to which a damaged surface layer affected the mechanical behavior was determined by the following experiment. A crystal was electroplated with a 0.8 micron coating of chromium. The chromium deposit was removed in hydrochloric acid and the crystal tested without further treatment. Figure 9 shows the stress-strain curve resulting from this test with curves for an unplated crystal and a coated crystal for comparison. It was found that a 0.8 micron chromium deposit damaged the substrate to a depth of approximately 15 microns.

The damaged surface layer produced by the above treatment was effective in raising the critical resolved shear stress and decreasing easy glide. However, the magnitude of the effect is considerably less than was observed when the coating was not removed prior to testing.

The influence of a damaged surface layer on mechanical behavior was further demonstrated using a copper crystal having a 125 Å evaporated chromium coating. The coating was applied to an unheated substrate and the thickness measured by the monitor resistance change technique. Coatings applied in this manner tend to be highly stressed. Figure 10a is a photomicrograph of the surface of the crystal after application of the coating by evaporation. A network of fine cracks is apparent. Removal of the coating in hydrochloric acid and subsequent dislocation etching revealed areas of high dislocation density associated with each of the cracks as shown in Figure 10b. At higher magnification (Figure 10c) individual dislocations produced by cracking of the coating were resolved. The distribution of dislocations was more uniform than produced by

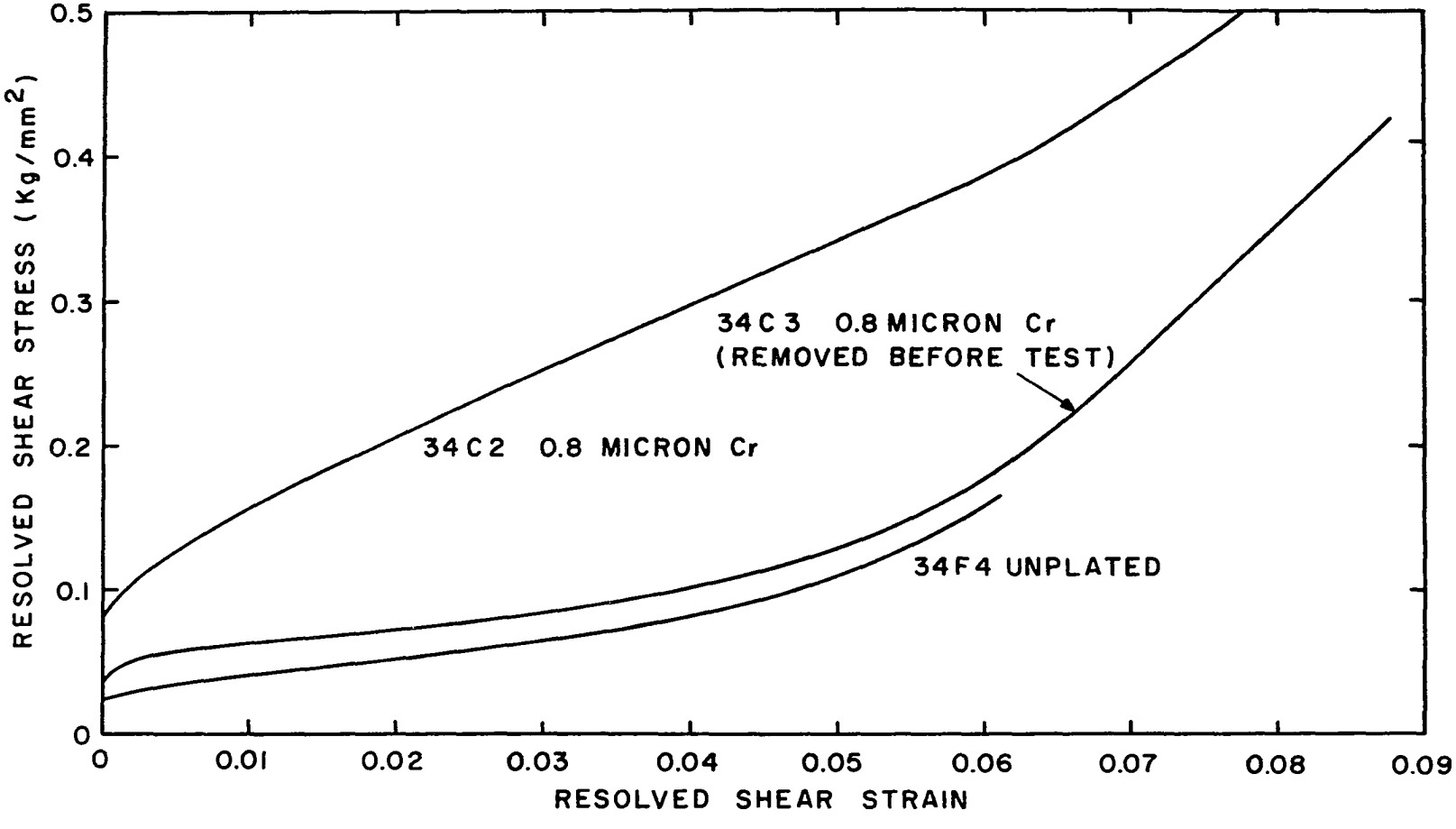


FIGURE 9

STRESS-STRAIN CURVE FOR A SPECIMEN ELECTROPLATED WITH 0.8 MICRON OF Cr AND THEN THE Cr REMOVED IN HCl BEFORE TESTING. An uncoated and a coated specimen are included for comparison.

cracking of the 0.5 micron chromium electro-deposit (Figure 8c). The depth to which the substrate was damaged by the 125 Å evaporated film was only about 2 microns.

The stress-strain curve for a crystal having a 125 Å evaporated chromium coating is shown in Figure 7. The flow stress throughout most of Stage I as well as the extent of easy glide are about the same as obtained from the specimen tested with only the damaged surface layer resulting from a 0.8 micron chromium electroplate. However, there were important differences which appear early in easy glide. The interpretation of these results requires consideration of the behavior of the coating during plastic deformation and therefore will be treated in the next section.

Figure 11 is a photomicrograph of the surface of a copper crystal which had been electroplated with a 1 micron coating of rhenium. The rhenium was removed in hydrogen peroxide and the specimen was lightly polished and etched to reveal dislocations. Less than 1 micron of copper was removed from the surface during polishing. The dislocation arrangement is typical of that observed in an annealed crystal. There is no indication of damage to the substrate crystal due to application of the coating. A 1 micron coating of rhenium did not produce a large strengthening effect (Figure 5).

Rhodium coatings applied directly to the copper crystals could not be removed conviently in order to observe the damage induced. A 1.7 micron rhodium film was applied to a portion of a copper crystal having a 500 Å coating of rhenium. Figure 12 is a photomicrograph of the surface of the copper after stripping the rhodium coating in

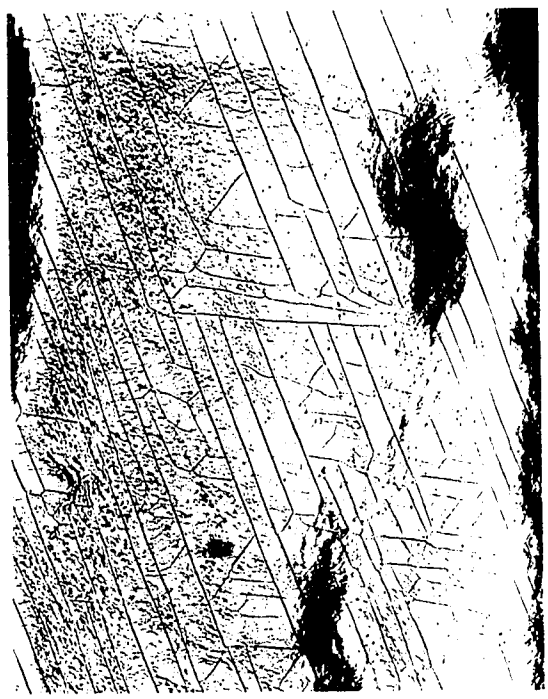


FIGURE 10a

SPECIMEN COATED WITH 125 Å Cr
BY VAPOR DEPOSITION. 50X

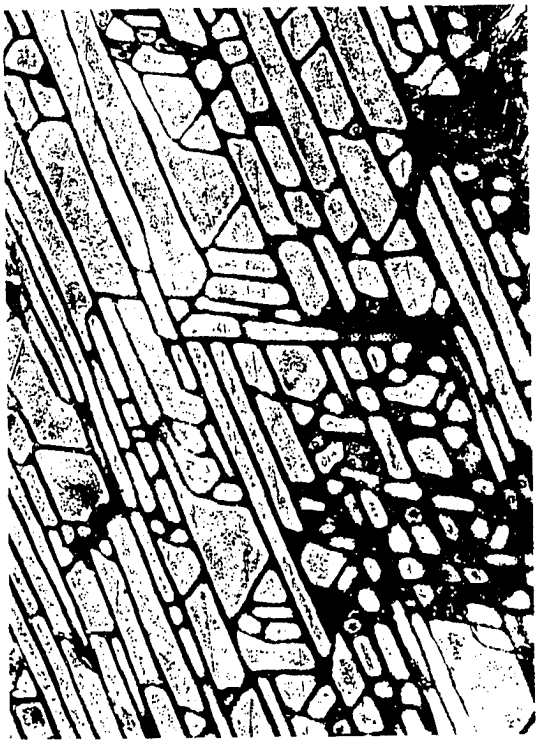


FIGURE 10b

SAME AREA AS IN FIGURE 10a AFTER Cr REMOVED IN HCl AND THE SPECIMEN REETCHED. 50X

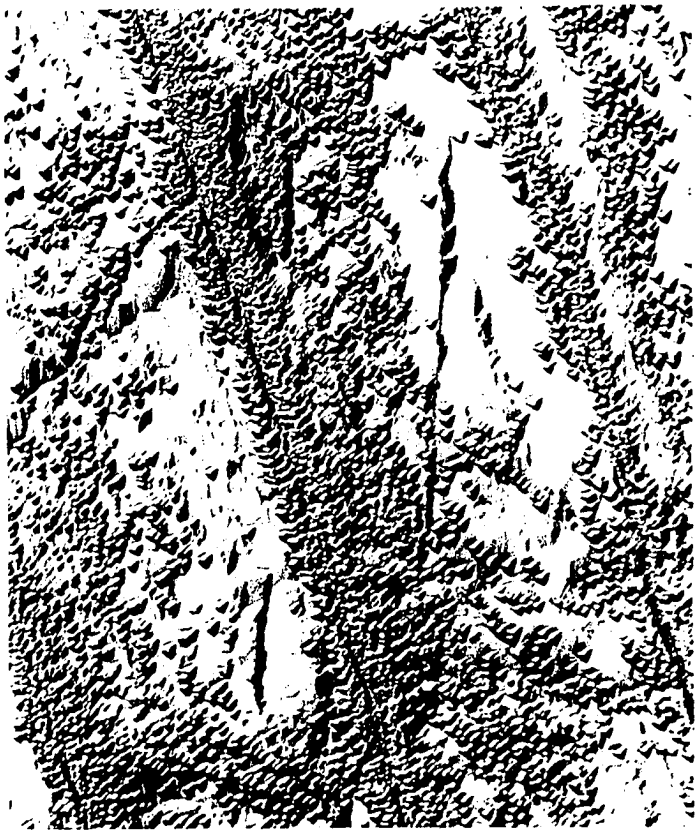


FIGURE 10c

HIGHER MAGNIFICATION OF SPECIMEN IN FIGURE 10b.
500X

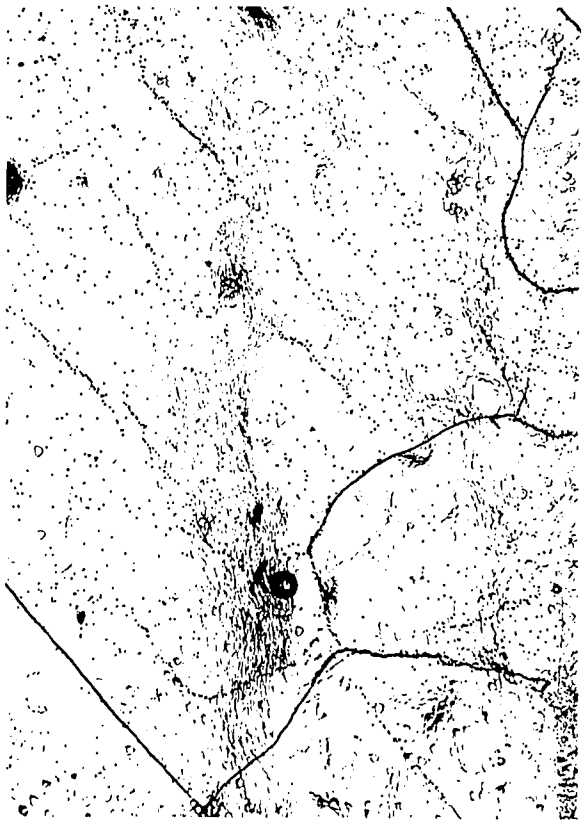


FIGURE 11

SURFACE OF A CRYSTAL ELECTROPLATED WITH A 1 MICRON COATING OF Re, THE COATING THEN REMOVED IN H_2O_2 AND THE CRYSTAL ETCHED TO REVEAL DISLOCATIONS. 50X

hydrogen peroxide and polishing the surface to a depth of 2 microns. The top of the micro shows the region of the crystal which was plated while the lower part shows an adjacent protected portion of the crystal. The underlying rhenium flash tends to shield the substrate from damage due to the rhodium coating. Nevertheless, a considerable degree of damage was induced by the rhodium film. The damaged layer extended to a depth of 25 microns. In order to provide a basis for comparison, a 1.7 micron chromium coating was applied over 500 Å of rhenium and removed by stripping. The degree of damage due to the chromium coating applied in this manner is shown in Figure 13. The depth of damage was about 12 microns.

Consideration of the state of residual stress in the coating seems to provide a basis for predicting which coatings may be expected to produce large strengthening effects. Measurements of the residual stresses made by the beam deflection method on 1 micron electro-deposits appear in Table 3. Chromium was the most highly stressed coating with rhodium next. Both were found to produce large strengthening effects (Figure 5). The residual stresses in other coatings (with the exception of ruthenium which showed too much scatter to be reliable) were significantly lower, as were the strengthening effects they produced.

A satisfactory treatment of the origin of residual stresses in electro-deposits and evaporated coatings is not to be found in the literature and, fortunately, is not essential to the discussion. However, certain features of presently accepted theoretical models can be considered. Van der Merwe (51) has attributed residual stresses in epitaxial films to lattice misfit between coating and substrate. Dislocations in the



FIGURE 12

DAMAGED SURFACE OF A CRYSTAL ELECTROPLATED WITH A 1.7 MICRON COATING OF Rh OVER A 500 Å FLASH OF Re. The plates were removed by stripping in H_2O_2 and the crystal then etched to reveal dislocations. 50X



FIGURE 13

DAMAGED SURFACE OF A CRYSTAL ELECTROPLATED WITH A 1.7 MICRON COATING OF Cr OVER A 500 Å FLASH OF Re. The plates were removed by stripping in H_2O_2 and the crystal then etched to reveal dislocations. 50X

interface introduce the elastic strains which are responsible for the stresses. Perhaps lattice misfit is also important in polycrystalline coatings as well although little is known about this situation.

Table 4 summarizes atomic sizes and the morphology of the various coatings used in this study. Typical Laue X-ray transmission patterns of the coatings in isolation appear in Appendix B. Coatings of copper, gold, and rhodium were epitaxial. Chromium showed a high degree of preferred orientation. The measurements of residual stresses in 1 micron electro-deposits made by the beam deflection method were not consistent with the lattice misfit criterion. Chromium, which indicated a high residual stress in tension, has only moderate misfit in a coordination number of 8 and zero misfit with 12 nearest neighbors. Rhodium, rhenium, and ruthenium would be expected to show residual compressive stress. However, tension was observed. Thus it would appear that the magnitude of the strengthening produced by a particular coating cannot be predicted on the basis of lattice misfit alone.

The results obtained in this study differ in some respects from those of Brame and Evans (13). Large lattice misfit does not seem inevitably to lead to brittle behavior of the coating. The electroplated gold coatings were epitaxial and showed slip line traces even though the lattice misfit was 11.3%. This lattice misfit is approximately twice the largest value used by Brame and Evans and, from their conclusions on the ability of dislocations to be injected into the film at large misfits, would be predicted to produce brittle behavior. Although lead showed slip line traces and its misfit with copper was 27%, the lead coatings were probably not epitaxial. Ruthenium with a misfit of 4.5% showed

TABLE 4

ATOMIC SIZES AND MORPHOLOGY OF COATINGS

Coating	Morphology	R* Å	R(12)# Å	$\frac{R_{Cu}-R^{**}_c}{R_c} \times 100$	$\frac{R_{Cu}-R(12)_c}{R(12)_c} \times 100$
Copper	Epitaxial	1.276	1.276	0.0	0.0
Lead	---	1.747	1.747	-27.0	-27.0
Gold	Epitaxial	1.439	1.439	-11.3	-11.3
Chromium	Preferred	1.247	1.276	2.33	0.0
Rhodium	Epitaxial	1.342	1.342	-4.91	-4.91
Ruthenium	---	1.322	1.336	-3.48	-4.50
Rhenium	---	1.367	1.373	-6.66	-7.06

* R = Radius of Atoms (Closest Approach)
\# R(12) = Radius of Atoms (Ligancy 12) as tabulated by Pauling (52)
** R_c = Radius of Coating Atoms

slip traces but epitaxial rhodium with a misfit of 4.9% exhibited brittle cracking. Chromium had small misfit with the copper, was not epitaxial, and exhibited cracking at low strains.

It is difficult to resolve these discrepancies with the very careful study of Brame and Evans. There were differences in experimental technique which may have affected the results. For example, the coatings used in this study were applied directly to the substrate crystal while in the previous study a thin flash of gold was used between substrate and coating. In the present work deformation involved only a single slip system and observations were made at relatively low strains. Brame and Evans gave no information about the orientation of their

specimens. However, the 15% extension which they used was a fairly severe deformation.

Behavior of the Coating during Deformation

The various coatings applied to copper crystals may be characterized by their adherence and tendency to crack during deformation. Rhenium coatings were observed to show gross detachment during Stage I. Figure 14a is a photomicrograph of the (111) surface of a crystal coated with 1 micron rhenium and strained to 8% shear. Detachment has occurred in a broad band roughly along the slip plane trace. Cracks in the coating generally ran parallel and normal to the tensile axis. It appeared that buckling preceded detachment of the coating. Figure 14b shows a portion of the previous micro at higher magnification. The arrow indicates a point at which buckling initiated. This type of behavior is strongly reminiscent of the observations of Edeleanu and Law (53) of anodized coatings on aluminum.

Crystals tested with coatings of ruthenium, lead, copper, and gold showed no cracks during deformation. Traces of the primary slip plane were observed on all surfaces. Figure 15 shows the surface of a ruthenium coated crystal after 4.5% shear. This appearance was typical for all of the above coatings. The presence of the coating did not significantly affect the slope or the extent of easy glide (see Figure 5). The minor increase in the flow stress during Stage I can be accounted for by the strength added due to the presence of the coating. Calculations were made to determine the required stress in the coating assuming only that the coating carries its portion of the load. In these



FIGURE 14a

(111) SURFACE OF A CRYSTAL COATED WITH 1 MICRON Re AND STRAINED TO 8% SHEAR. 50X

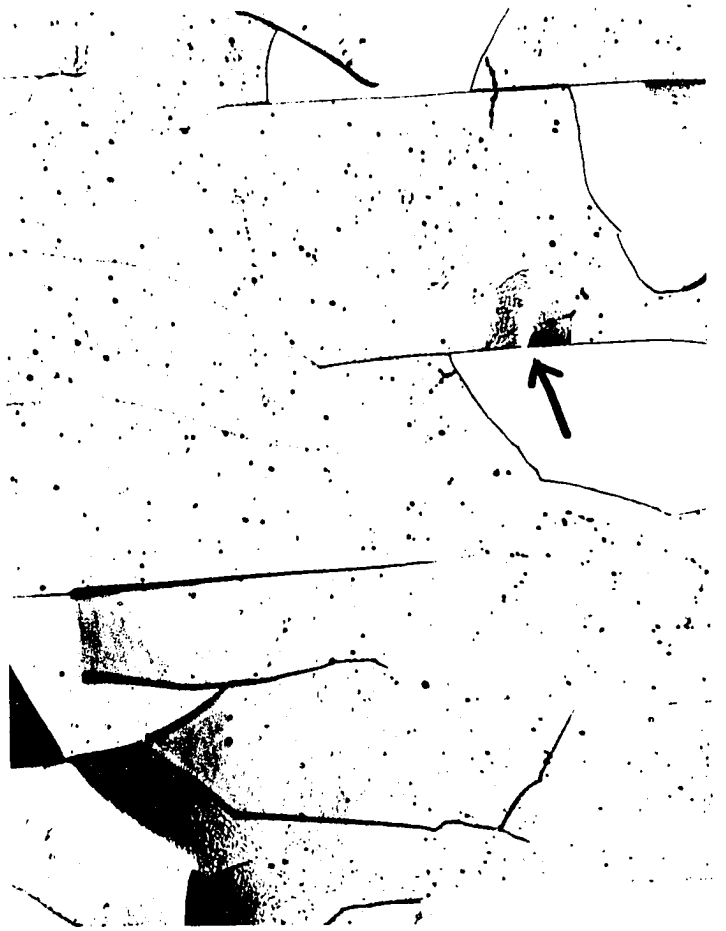


FIGURE 14b

HIGHER MAGNIFICATION OF SAME AREA SHOWN IN FIGURE 14a.
500X

calculations the stress was determined by taking the difference between loads in plated and unplated specimens at a given strain and dividing this difference by the cross sectional area of the coating. The results of these calculations made at several strains in Stage I for various coatings are plotted in Figure 16. Considering that thin flims may be several times stronger than bulk material, these stress levels are not large enough to require that a film-substrate interaction be evoked, i.e., the strength added by coating a crystal with ruthenium, lead, copper, or gold may be explained by the strength of the thin film itself.

Lead coatings were removed from the copper crystals in hydrogen peroxide. There was no evidence of surface damage either prior to or during deformation. The other coatings, gold, copper, and ruthenium could only be removed when they were applied over a 500 Å flash of rhenium. The observation of no surface damage with these coatings applied in this manner is considered less reliable because the relatively strong rhenium underplate may have shielded the crystal surface from the effects of deformation of the coating.

Chromium coatings cracked transverse to the tensile axis at shear strains of less than 10^{-3}. This cracking is believed to be a result of the superposition of the applied tensile stress and the residual stresses already present in the coating as a result of its formation. Figure 17a is a photomicrograph of a specimen which was coated with 1 micron of chromium and strained to 2×10^{-3} in shear. The coating was dissolved and about 1 micron of copper was removed by chemical polishing prior to dislocation etching. Damage due to cracks in the coating which were transverse to the tension axis is apparent. The density and distribution



FIGURE 15

SURFACE OF A CRYSTAL COATED WITH 1 MICRON OF Ru AND STRAINED TO 4.5% SHEAR. 500X

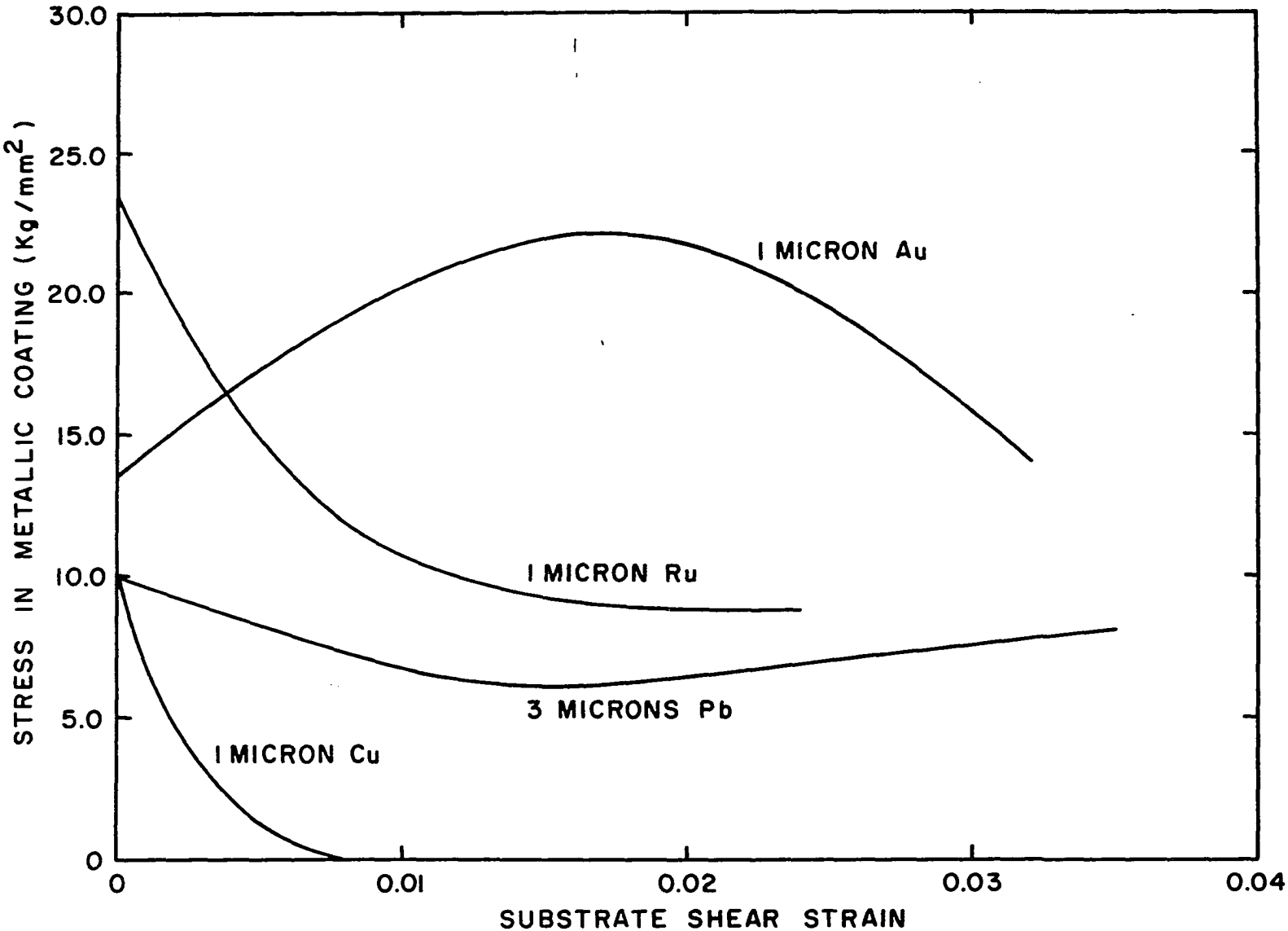


FIGURE 16

CURVES SHOWING THE STRESS LEVELS IN THE VARIOUS COATINGS
AS A FUNCTION OF SUBSTRATE SHEAR STRAIN

of these cracks are different from those observed in the unstrained condition (Figure 8). Therefore, they are considered to have resulted from the deformation. Figure 17b shows the same specimen at higher magnification. Individual dislocation etch pits which make up the crack induced damage are apparent. With increasing deformation the density of cracks in the coating increased thus increasing the amount of surface damage.

The localized increase in dislocation density that was observed in this experiment could only have resulted from cracking of the coating. The dislocations were generated at the surface by shear which accompanied the release of residual stresses in the coating. The regions of high density are not generally parallel to slip plane traces and therefore are not evidence of pile-ups. These regions of high dislocation density induced at 2×10^{-3} shear extended to a depth of about 7 microns.

It was determined that this same process occurs in many of the coatings which do not crack spontaneously as a result of residual stresses alone. As previously discussed 1 micron rhenium coatings did not produce sufficient residual stresses to cause spontaneous cracking and damage of the substrate (see Figure 11). An experiment similar to that discussed above was carried out with a specimen having a 1 micron rhenium coating. The specimen was strained 2×10^{-3} in shear and then the coating was removed. Figure 18a shows the (111) surface after removal of about 1 micron of copper and subsequent dislocation etching. The damage induced by cracking of the coating is clearly visible on the right hand side of the photomicrograph. This region was near one edge of the specimen. At higher magnification (Figure 18b) individual dislocation etch pits were



FIGURE 17a

SUBSTRATE DAMAGE BENEATH THE CRACKS IN A 1 MICRON Cr FILM. The specimen was strained to 2×10^{-3} in shear, the coating removed in HCl and the copper surface etched to reveal dislocations. 50X



FIGURE 17b

SAME SPECIMEN AS SHOWN IN FIGURE 17a AT HIGHER MAGNIFICATION.
500X

revealed. The damage induced by this film rupture at 2×10^{-3} shear was shallow extending about 3 microns in depth and involving only a small portion of the surface area of the specimen. As the specimen was strained further, detachment occurred on the (111) face.

The difference between the flow stresses of uncoated crystals and crystals having coatings which were observed to crack during deformation involves the influence of the damaged surface layer. The stress-strain curves for crystals having 1 micron coatings of rhodium or chromium show high flow stress and high strain hardening rates relative to the uncoated crystal. This is a combination of progressively increasing surface damage due to film rupture during deformation and the load carrying contribution of the coatings. Both of these coatings have very high hardnesses indicating significant film strength.

Figure 9 provides sufficient data for an estimate of the film strength of the 0.8 micron chromium coating. At zero extension the difference between the load carried by the coated specimen and the specimen which had its coating removed before testing was approximately 1.7 lbs. This load difference corresponds to a stress of 108,000 psi in the coating, a value which is not unreasonably large. Similar calculations cannot be made at strains greater than zero since film cracking increases the amount of surface damage in the coated specimen.

The behavior of the specimen having a 125 Å chromium vapor deposit also must be interpreted in terms of film rupture during deformation. Figure 19 shows tracings of the initial portions of the load-extension curves as plotted directly by the Instron machine for all the specimens represented in figures 7 and 9. Variations in dimensions among specimens

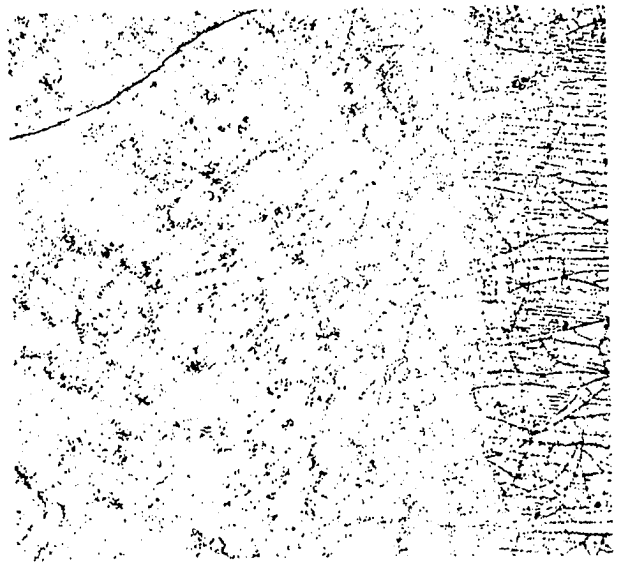


FIGURE 18a

SUBSTRATE DAMAGE BENEATH CRACKS IN A 1 MICRON Re FILM. The specimen was strained to 2 x 10^{-3} in shear, the coating removed in H_2O_2 and the copper surface etched to reveal dislocations. 50X



FIGURE 18b

SAME SPECIMEN AS SHOWN IN FIGURE 18a AT HIGHER MAGNIFICATION.
500X

were small and therefore the stress-strain behavior for these specimens may be compared using the curves of Figure 19. The specimen tested with a 125 Å vapor deposit showed a flow stress at the onset of plastic deformation approximately equivalent to the flow stress in an uncoated crystal. However, the initial strain hardening rate is about the same as observed with a 0.8 micron coating of chromium. As plastic deformation continues, the flow stress quickly levels off at about the same value obtained with just the damaged layer resulting from the 0.8 micron chromium electrodeposit.

The vapor deposit exhibited fine cracks prior to deformation (Figure 10). This caused a shallow layer of surface damage. The strength of the coating and the layer of damage did not make a significant contribution to the flow stress at the elastic limit. However, further cracking of the coating accompanied the onset of plastic deformation. The initial portion of Stage I was characterized by a high slope reflecting the increasing damage and high strain hardening rate at the surface. There was evidence that the vapor deposited coating tended to exhibit gross detachment as deformation of the substrate proceeded. It is believed that the coating lost its effectiveness in producing damage at the surface when the load-extension curve became parallel to the curve for the uncoated specimen.

Figure 20 shows the surface of a crystal tested with the vapor deposit of chromium after deformation into Stage III. Gross detachment is evident. This behavior is in contrast to the observations of the behavior of electro-deposits after considerable deformation. Figure 21 shows a surface typical of a 1 micron chromium plated crystal deformed

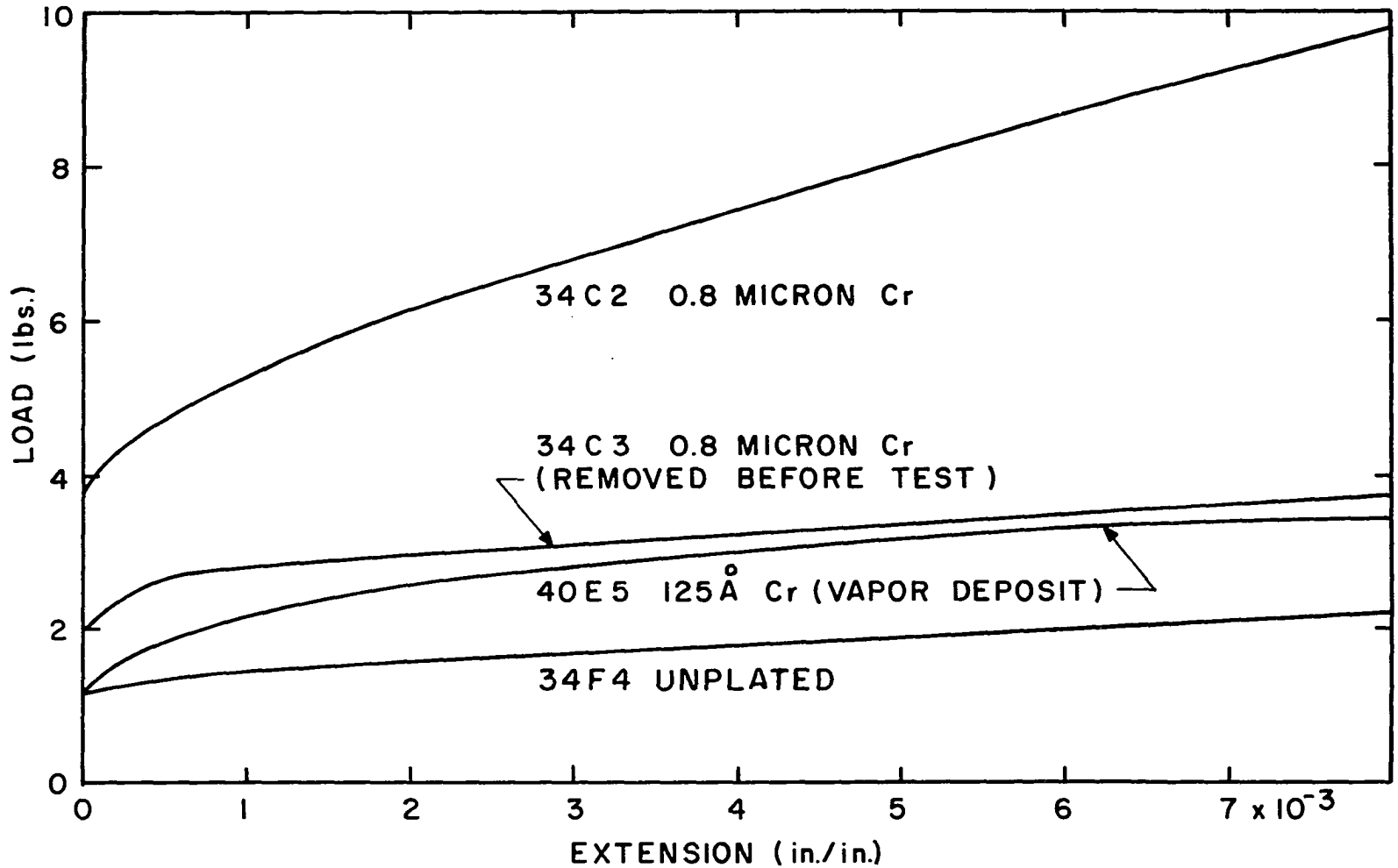


FIGURE 19

LOAD-EXTENSION CURVES FOR A SPECIMEN WITH A 125 Å VAPOR DEPOSITED Cr COATING, A SPECIMEN WITH A 0.8 MICRON ELECTROPLATED Cr COATING WHICH WAS REMOVED BEFORE TESTING, A SPECIMEN WITH A 0.8 MICRON ELECTROPLATED Cr COATING, AND AN UNPLATED SPECIMEN

into Stage III. The network of cracks was extremely fine indicating continued cracking throughout deformation of the substrate. However, no detachment was observed. Thus continual cracking might be expected to produce continual deformation of the sub-surface layer contributing to the strengthening of the substrate crystal. The decreasing rate of work hardening throughout plastic deformation is consistent with the continued decrease of the strength contribution made by the coating as it continually cracks.

The layer of surface damage caused by cracking of the vapor deposit during deformation causes a strengthening effect which is about equivalent to that resulting from spontaneous cracking of the 0.8 micron chromium coating. Of particular importance is the observation that the strain hardening rate for both during most of Stage I is the same as in the uncoated crystal. It must be concluded that in these two situations the surface damage causes no significant change in the strain hardening of the remainder of the crystal. Therefore in these cases it seems inappropriate to presume that dislocations generated within the undamaged substrate are greatly impeded in their motion through the crystal or toward the surface by the damaged layer. Likewise, these stress-strain curves seem to rule out the possibility that the layer of damage thickened rapidly as plastic deformation proceeded.

The observation that neither the thin vapor deposit nor the damaged layer from a 0.8 micron chromium coating was able to affect the strain hardening rate in Stage I must be a result of the type of surface damage which was produced. After application and deformation the vapor deposit of chromium produced a very thin layer of damage which was relatively

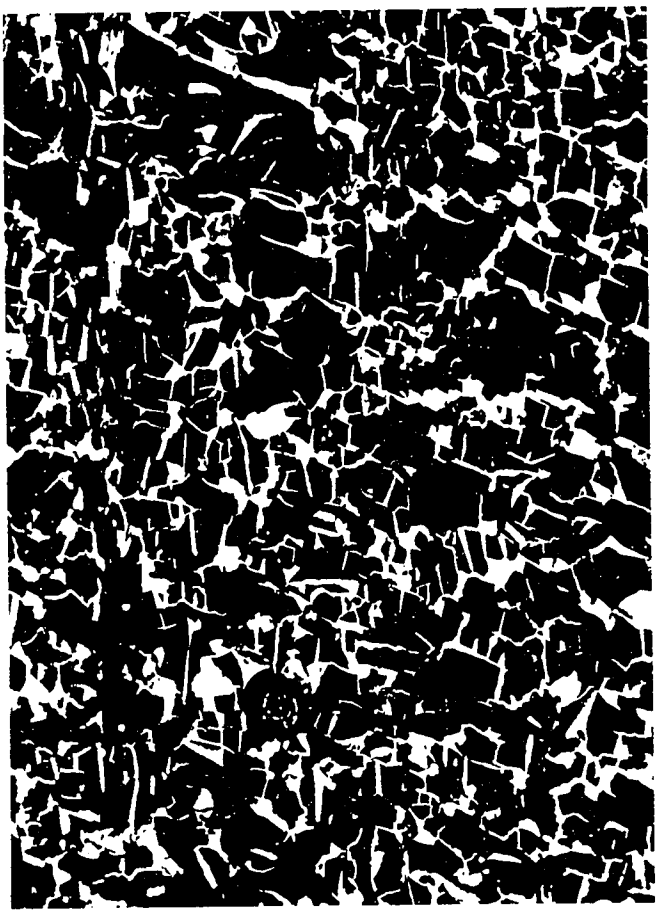


FIGURE 20

SURFACE OF A CRYSTAL TESTED INTO STAGE III
WITH A 125 Å VAPOR DEPOSIT OF Cr. 50X

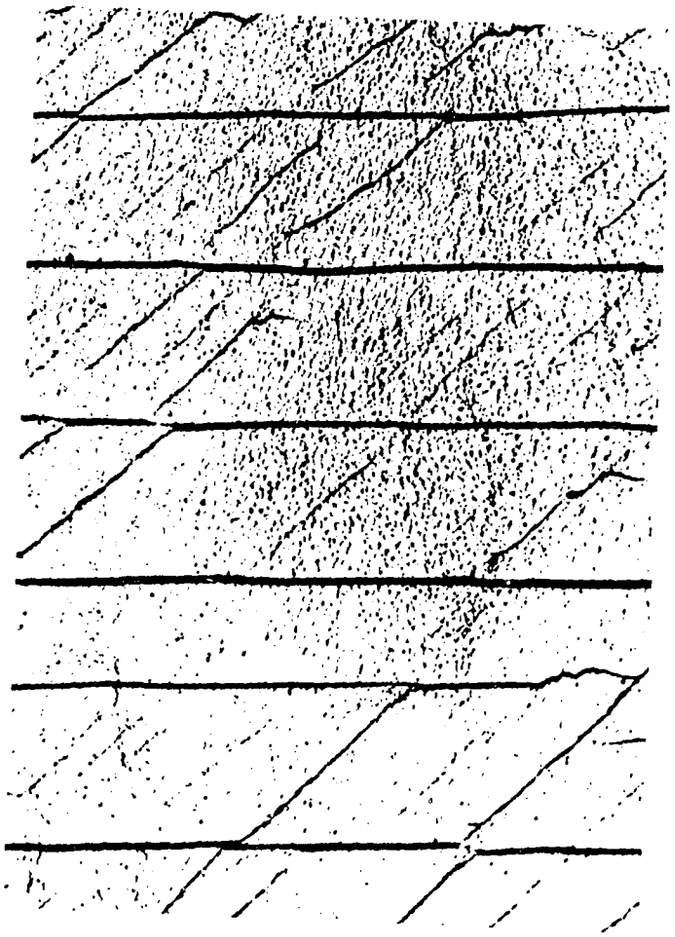


FIGURE 21

SURFACE OF A CRYSTAL TESTED INTO STAGE III WITH A 1 MICRON Cr ELECTROPLATE. 500X

intense. However, because of its thinness, it was transparent to the passage of dislocations moving toward the surface. The layer of damage which resulted from only the application of the 0.8 micron chromium coating was relatively thick but not sufficiently intense to impede a major portion of the dislocations moving toward the surface. Therefore, this damaged layer is also relatively transparent to the motion of dislocations moving toward the surface.

The damaged surface layer produced by Nakada and Chalmers as a result of micropeening gold crystals (34) had a greater depth of damage than any observed in the present study. To be sure, the extent of the easy glide is a rather small portion of their stress-strain curves. However, careful examination of the stress-strain curves which were presented indicate an increase in slope at a strain of about 0.5%. Thus Stage I was not completely suppressed by the damage in either their experiments or the ones of this study. The surface regions of a damaged crystal deform with strain hardening rates characteristic of Stage II or III while the crystal interior exhibits easy glide. The strain hardening rate observed at a given strain during plastic deformation reflects an averaging of these different rates. A change in strain hardening rate of coated crystals as a function of strain (at low strains) may be expected to arise from several sources. Continual cracking of the coating considerably increases the dislocation density of the surface layer. An additional increase in the dislocation density of the surface layer arises from plastic deformation due to the applied stresses. Both of these factors are reflected in the strain hardening rate. The likelihood that the damaged layer changes in thickness as deformation proceeds must be

admitted. Thus the relative proportions of damaged and undamaged material change, which also affects the strain hardening rate.

Block (16) has reported that the extent of Stage I for crystals having chromium coatings from 0.1 to 3 microns thick decreases with increasing coating thickness. The stress-strain curves of Figure 22 were taken from this work and illustrate the effect. This regular decrease in extent of easy glide must be interpreted in terms of thickening of the damaged layer as deformation proceeds.

Surface damage, whether a result of spontaneous cracking of the coating or cracking during deformation, may be expected to produce strengthening effects. Dislocation multiplication will occur on several slip systems causing dislocation tangles near the surface. Further deformation near the surface is accomplished by the operation of other slip systems in addition to the primary slip system. The damaged layer may thus tend to propagate deeper into the substrate crystal. Deformation of the undamaged portion of the substrate proceeds by the generation of dislocations on the primary slip systems which move toward the surface. These dislocations are impeded by the tangled layer and the tendency to form new tangles with dislocations generated near the surface and moving inward.

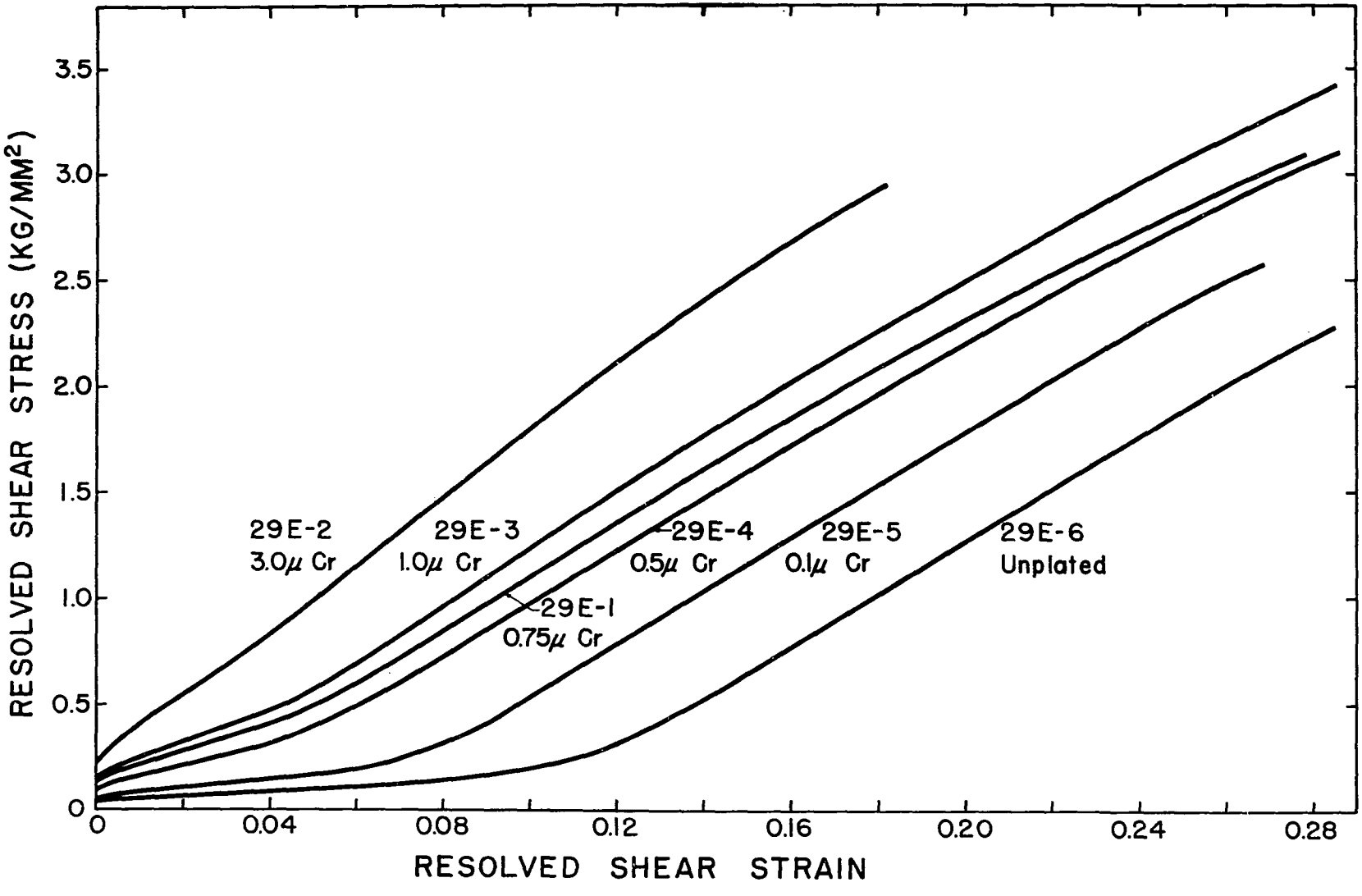


FIGURE 22

STRESS-STRAIN CURVES FOR SPECIMENS OF THE SAME CRYSTAL
HAVING Cr COATINGS OF VARIOUS THICKNESSES
(After Block)-(16)

CHAPTER IV

CONCLUSIONS

In the absence of a regular dependence of the strengthening effect upon coating strength, a simple pile-up of dislocations at the coating-substrate interface appears not to be a process of major importance. Observations of specimens which were strained and etched to reveal dislocations show no singularities at the interface which suggest the operation of such a mechanism.

The lack of dependence upon the shear modulus of the coating precludes the elastic repulsion of dislocations from the coating-substrate interface as an important process in producing the observed film strengthening. Similarly there was no indication that the suppression of surface dislocation sources is an important consideration.

The observation that a large strengthening effect was always accompanied by film cracking either prior to or during deformation suggests that residual stresses in the coating originate the effect. At the location of each crack localized deformation extending from the surface into the substrate was noted. The cracks form spontaneously during formation of the film or when external stresses sufficient to cause rupture are superimposed upon the residual coating stresses.

It is suggested that the major portion of the strengthening effect traditionally attributed to the presence of a surface coating is caused by a damaged surface layer.

BIBLIOGRAPHY

1. I. R. Kramer and J. Demer; Prog. Mat. Science (1961) 9, 131.

2. E. S. Machlin; Strengthening Mechanisms in Solids, A.S.M. Cleveland (1962), 375.

3. R. Roscoe; Nature (1934), 133, 912.

4. A. H. Cottrell and D. F. Gibbons; Nature (1948), 162, 488.

5. J. Takamura; Mem. Fac. Eng. Kyoto Univ. (1956), 18 (3), 255.

6. R. L. Fleischer and B. Chalmers; Trans. Met. Soc. A.I.M.E. (1958), 212 (2), 265.

7. S. Harper and A. H. Cottrell; Proc. Phys. Soc. (1950), B63, 331.

8. E. N. da C. Andrade and C. Henderson; Phil. Trans. Roy. Soc. (1951), A 244, 177.

9. J. J. Gilman and T. A. Read; Trans. Met. Soc. A.I.M.E. (1952), 194, 875.

10. J. J. Gilman; A.S.T.M. STP No. 171, Phila., Pa. (1955), 3.

11. M. R. Pickus and E. R. Parker; Trans. Met. Soc. A.I.M.E. (1951) 191, 792.

12. F. R. Lipsett and R. King; Proc. Phys. Soc. (1957), (B) 70 (6), 608.

13. D. R. Brame and T. Evans; Phil. Mag. (1958), (viii) (33) 3, 971.

14. J. Garstone, R. W. K. Honeycombe, and G. Greetham; Acta Met. (1956), 4, 485.

15. F. D. Rosi; Acta Met. (1957), 5, 348.

16. R. J. Block; Ph.D. Thesis (1963), Univ. of Illinois.

17. C. S. Barrett; Acta Met. (1953), 1, 2.

18. C. S. Barrett, P. M. Aziz, and I. Markson; Trans. Met. Soc. A.I.M.E. (1953), 197, 1655.

19. D. B. Holt; Acta Met. (1962), 10, 1021.

20. A. K. Head; Proc. Phil. Mag. (1953), 44, 92.

21. A. H. Cottrell; Dislocations and Plastic Flow in Crystals, Clarendon Press, Oxford (1953), 55.

22. A. Seeger; Dislocations and Mechanical Properties of Crystals, Wiley, New York, (1957), 243.

23. L. M. Clarebrough and M. E. Hargreaves; Prog. in Metal Phys. (1959), 8, 1.

24. J. Friedel; Dislocations, Addison-Wesley (1964), 258.

25. F. W. Young, Jr.; J. Appl. Phys. (1961), 32, 1815.

26. J. C. Fisher; Trans. Met. Soc. A.I.M.E. (1952), 194, 531.

27. M. A. Adams; Acta Met. (1958), 6, 327.

28. J. J. Gilman; Phil. Mag. (1961), 6, 159.

29. I. R. Kramer and L. J. Demer; Trans. Met. Soc. A.I.M.E. (1961), 221, 780.

30. I. R. Kramer; Trans. Met. Soc. A.I.M.E. (1961), 221, 989.

31. I. R. Kramer; Trans. Met. Soc. A.I.M.E. (1965), 233, 1562.

32. K. Kolb and E. Macherauch; Phil. Mag. (1962), 7, 415.

33. K. Sumino; J. Phys. Soc. Japan (1962), 17, 454.

34. Y. Nakada and B. Chalmers; Trans. Met. Soc. A.I.M.E. (1964), 230, 1339.

35. J. Diehl; Z. Metallk. (1956), 47, 331.

36. J. Diehl; Z. Metallk. (1956), 47, 411.

37. S. Mader; Z. Physik (1957), 73, 149.

38. J. D. Livingston; Acta Met. (1962), 10, 230.

39. M. J. Hordon; Acta Met. (1962), 10, 999.

40. F. W. Young; J. Appl. Phys. (1962), 33, 963.

41. N. F. Mott; Phil. Mag. (1952), 43, 1151.

42. H. Suzuki, S. Ikeda, and S. Takeuchi; J. Phys. Soc. Japan (1956), 11 382.

43. L. C. Lovell and J. H. Wernick; J. Appl. Phys. (1959), 30, 590.

44. F. W. Young, Jr.; J. Appl. Phys. (1961), 32, 192.

45. J. D. Livingston; J. Appl. Phys. (1960), 31, 1071.

46. A. K. N. Reddy and H. Wilman; Trans. Inst. of Metal Finishing (1958), 36, 97.

47. E. Schmid and W. Boas; Kristallphastizitat (1935), Springer-Verlag, Berlin.

48. A. Brenner and S. Senderoff; J. Res. National Bureau of Standards (1949), 42, 105.

49. T. Evans and D. R. Schwarzenberger; Phil. Mag. (1959), 4, 899.

50. A. R. C. Westwood; Phil. Mag. Ser. 8 (1960), 5, 981.

51. J. H. van der Merwe; Phil. Mag. (1962), 7, 1433.

52. L. Pauling; The Nature of the Chemical Bond (1960), Cornell University Press, 403.

53. C. Edeleanu and T. J. Law; Phil. Mag. (1962), 7, 573.

APPENDIX A

STRESS-STRAIN PARAMETERS FOR COATED AND UNCOATED CRYSTALS

Crystal	Cross Sectional Area mm^2	$\tau_{00\ obs}$ gm/mm^2	τ_0 gm/mm^2	a_2 cm/cm	τ_2 gm/mm^2	θ_I gm/mm^2
33F3	9.10	31.3	36	0.0529	110	1400
34B5	9.37	38.6	50	0.0615	156	1590
34C1	9.91	22.6	25	0.0937	112	845
34C2	9.84	80.2	118	0.0678	408	4430
34C3	10.00	43.9	52	0.0543	109	1080
34D5	9.37	22.2	-	-	-	-
34F1	9.84	34.5	71	0.0597	272	3400
34F4	10.00	25.9	27	0.0557	96	1230
35F2	10.16	45.6	50	0.0456	113	1400
35F4	9.83	61.7	65	0.0432	137	1650
38B3	9.30	40.6	44	0.0626	104	1060
38C2	9.44	40.3	45	0.0579	119	1350
38E2	9.92	44.9	52	0.0589	150	1820
40E2	9.76	34.0	38	0.0385	84	1200
40E5	9.84	23.0	59	0.0518	110	985

Crystal	Surface Condition	$\tau_{00\ cal}$ gm/mm^2	$\tau_{00\ obs} - \tau_{00\ cal}$ gm/mm^2	$\tau_0 - \tau_{00\ cal}$ gm/mm^2	$\theta_I/\theta_{I\ ave}$
33F3	Unplated	32.3	1.0	3.7	0.91
34B5	1 micron Au	27.2	11.4	22.8	1.37
34C1	Unplated	25.0	-2.4	2.4	0.73
34C2	0.8 micron Cr	27.0	53.2	37.8	3.80
34C3	0.8 micron Cr Removed	38.1	5.8	13.9	0.93
34D5	Unplated	22.2	0.0	-	-
34F1	1 micron Rh	19.3	15.2	51.7	2.92
34F4	Unplated	22.7	3.2	4.3	1.05
35F2	3 microns Pb	31.4	14.2	18.3	1.20
35F4	Unplated	61.7	0.0	3.3	1.42
38B3	Unplated	38.1	2.5	5.9	0.91
38C2	1 micron Ru	24.4	15.9	20.6	1.16
38E2	1 micron Re	24.1	20.8	17.9	1.56
40E2	1 micron Cu	26.8	7.2	11.2	1.03
40E5	125 Å Cr Vapor-Deposited	26.8	5.2	32.2	0.84

APPENDIX B

The morphology of several of the coatings of this study was examined by X-ray diffraction techniques. This examination was made after the coatings were electroplated on a (111) face of a copper crystal and then isolated from the substrate. The sharpness of the reflections and absence of diffraction rings were taken as indications of the degree to which epitaxy was achieved.

A Laue back reflection X-ray pattern of the (111) face of an uncoated copper crystal is shown in Figure B1. Figure B2 is the diffraction pattern taken in transmission of an isolated 1 micron Rh electro-deposit. The strong, six fold symmetry indicates a tendency to form epitaxy with the copper substrate. The additional reflections which also show (111) symmetry indicate a second lattice parameter different from the substrate copper. The several faint diffraction rings may have been caused by residues on the isolated coating and are not considered of sufficient intensity to indicate any structural aspects of the coating.

Figure B3 is a Laue transmission pattern from a 1 micron gold electro-deposit. There are strong (111) reflections evident. In addition, portions of the diffraction rings are visible. This pattern suggests a tendency to form epitaxy with the copper substrate. Where epitaxy does not occur, the coating forms large grains having a strongly preferred orientation similar to the substrate.

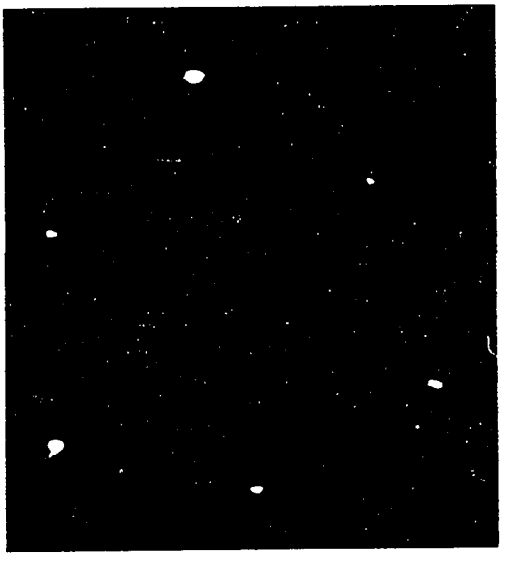


FIGURE B1

LAUE BACK REFLECTION X-RAY PATTERN OF THE (111) FACE OF AN UNCOATED COPPER CRYSTAL.



FIGURE B2

LAUE TRANSMISSION X-RAY PATTERN OF A 1 MICRON RHODIUM ELECTRO-DEPOSIT IN ISOLATION.

Figure B4 is the Laue transmission pattern for a 1 micron chromium electro-deposit. The presence of broad rings with intensity peaks having six fold symmetry suggest a coating which is fine grained polycrystalline having a (111) preferred orientation.

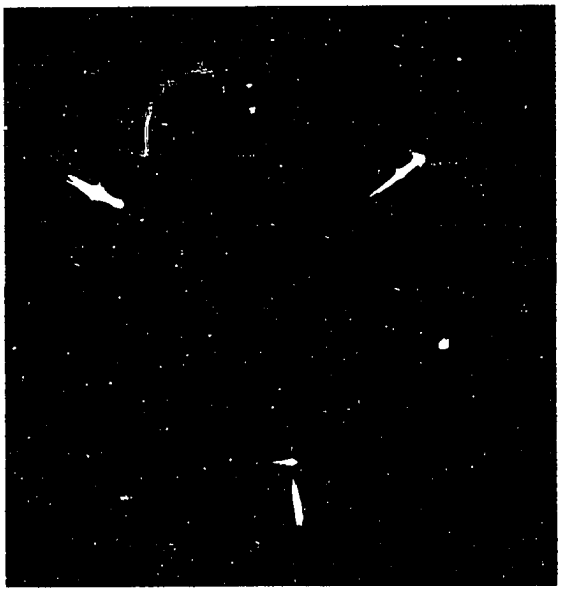


FIGURE B3

LAUE TRANSMISSION X-RAY PATTERN OF A 1 MICRON GOLD ELECTRO-DEPOSIT IN ISOLATION.

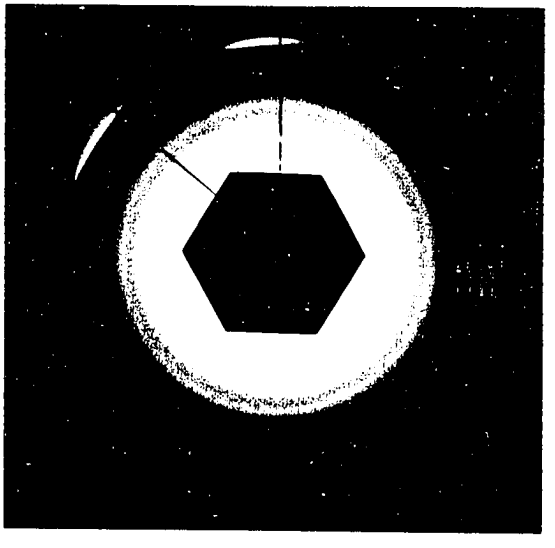


FIGURE B4

LAUE TRANSMISSION X-RAY PATTERN OF A 1 MICRON CHROMIUM ELECTRO-DEPOSIT IN ISOLATION.